北京師範大學
BEIJING NORMAL UNIVERSITY

遥感数据的时空相关性及在数据预处理中应用

报告人：**陈　晋**

北京师范大学地表过程与资源生态国家重点实验室

北京师范大学减灾与应急管理研究院

2012年12月10日

目录

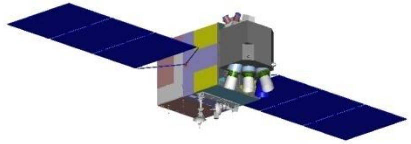

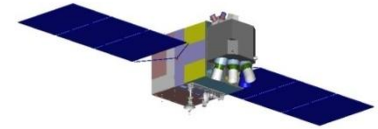

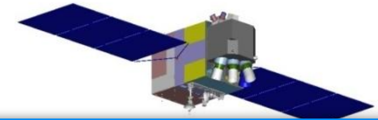

1 遥感数据的时空相关性

遥感数据目前已经被地理学、生态学等诸多领域作为大尺度

不同于普通的数字图像处理，遥感数据的处理过程中，需要考虑遥感数据的**时空相关性**，杜绝将数据孤立地处理。

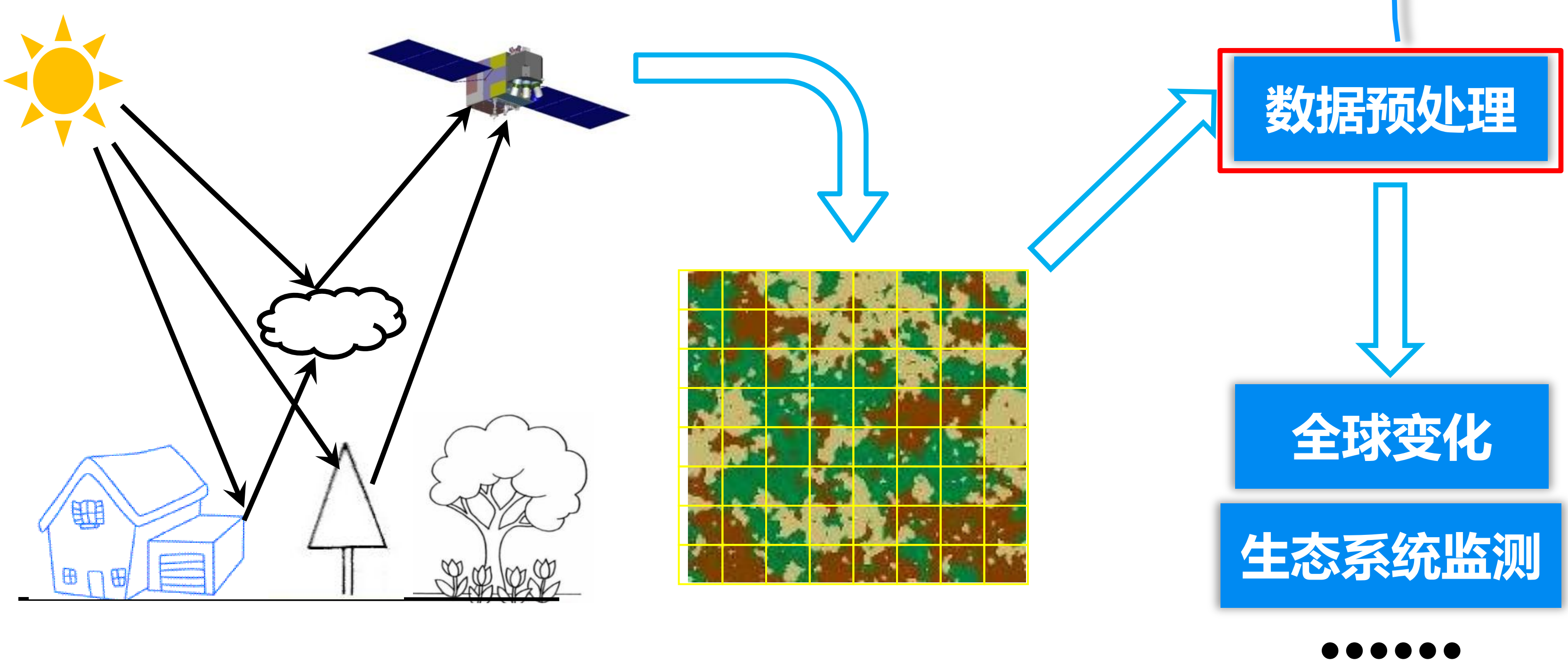

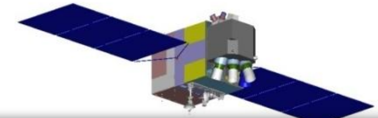

1 遥感数据的时空相关性

空间相关性 *Rs*

“All attribute values on a geographic surface are related to each other, but **closer values** are **more strongly related** than more distant ones.” —— Tobler’s First Law

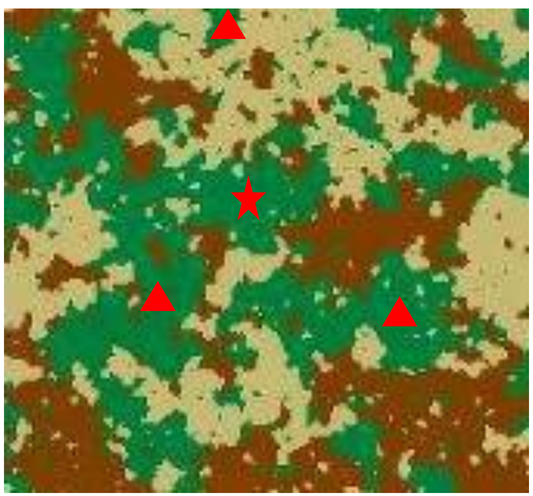

$$R_s(i,j) = \underbrace{f}_{\text{相关函数}}(\underbrace{d(i,j)}_{\text{距离因子}}|\underbrace{c(i,j)}_{\text{类别因子}})$$

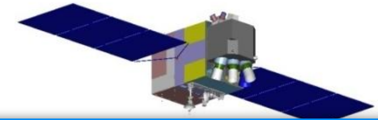

1 遥感数据的时空相关性

时间相关性 *Rt*

地物的部分属性会随着时间的推移发生周期或者非周期性的变化，这些连续的变化便形成了地物的时间相关性。间隔时间越短，地物属性应该越接近。

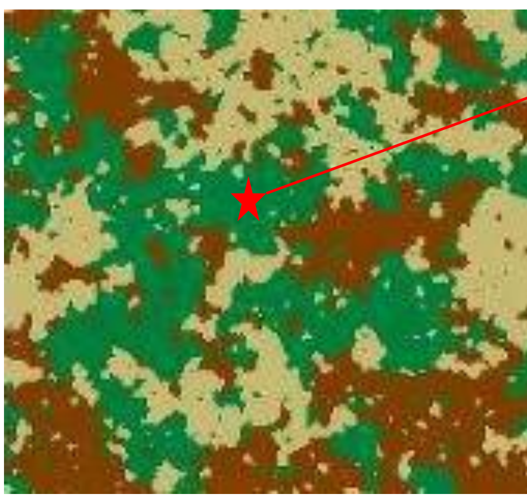

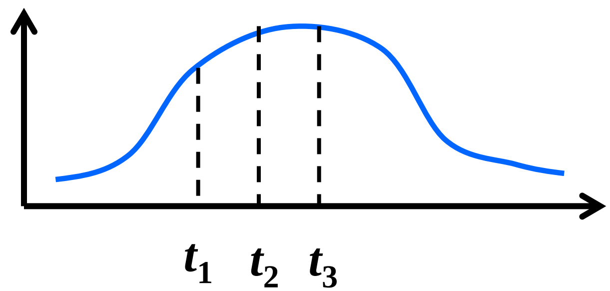

$$R_t(t_i, t_j) = \underbrace{f}_{\text{相关函数}}(\underbrace{\Delta t}_{\text{距离因子}}|\underbrace{c(pixel)}_{\text{类别因子}})$$

1 遥感数据的时空相关性

空间相关性的时间不变效应

在自然情况下若地物类型不变，地物的空间相关性应该是不随时间的推移而发生变化。

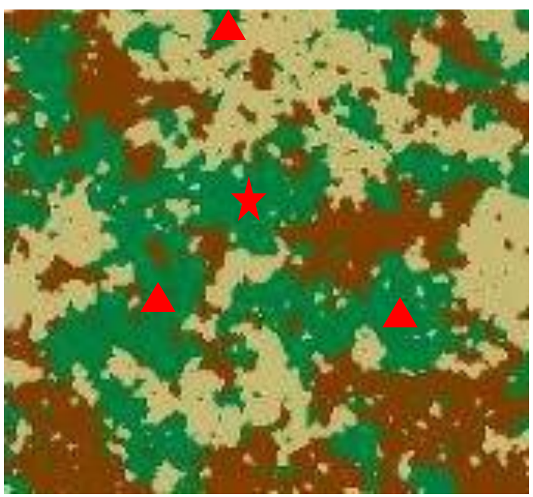

$$R_s(i,j,t_k) = R_s(i,j,t_l)$$

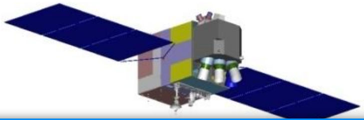

1 遥感数据的时空相关性

混合像元分解

由于地物覆盖类型的复杂性和传感器分辨率的限制，混合像元在遥感数据中十分普遍，混合像元分解即是获得混合像元中各地物类型比例的一种重要方法。

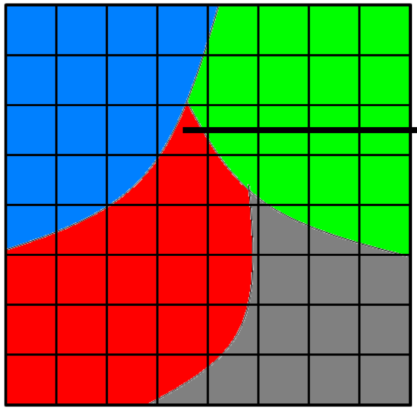

端元比例

$$R_{mix} = \sum_i f_i R_i + \varepsilon$$

混合光谱

端元光谱

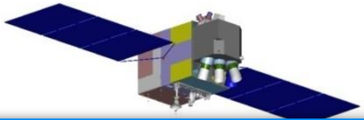

1 遥感数据的时空相关性

数据缺失问题

由于多方面因素的限制，遥感数据的缺失问题是遥感数据预处理中面临的最主要的问题。

- 数据缺失
  - 已有时相数据缺失
    - 条带(ETM+)
    - 厚云
    - 山体阴影
  - 特定时相数据缺失
    - 回访周期

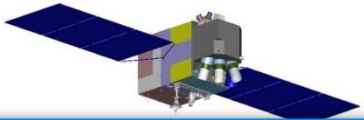

1 遥感数据的时空相关性

对于数据缺失问题，其根本的解决方法是充分利用遥感数据的时空相关性根据已有数据进行插值。

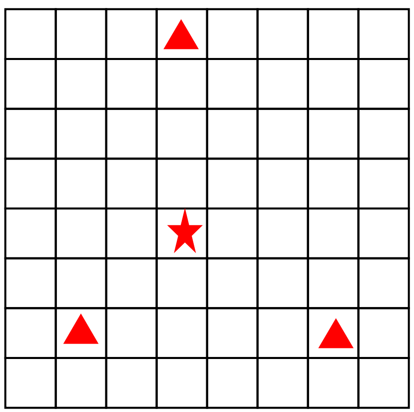

★ 目标像元

▲ 相似像元

$$R=\sum_{t}\underbrace{w_t}_{\text{时间相关}}\sum_{i}\underbrace{w_i}_{\text{空间相关}}\underbrace{R_{i,t}}_{\text{相似像元}}$$

时间相关

相似像元

空间相关

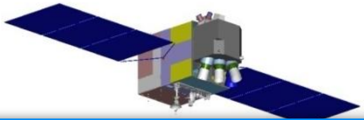

1 遥感数据的时空相关性

1. 寻找相似像元
2. 确定权重
3. 确定插值函数

$\min D(i,j)$ 时间、空间、特征

$w=f(D(i,j)|t,s)$

时间、空间、特征

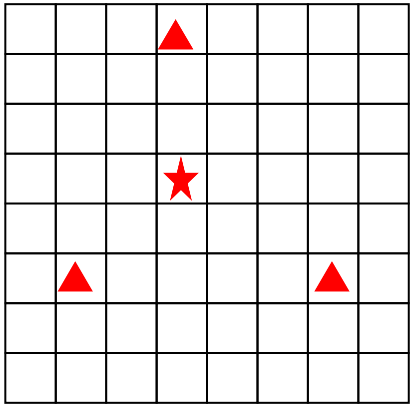

★ 目标像元

▲ 相似像元

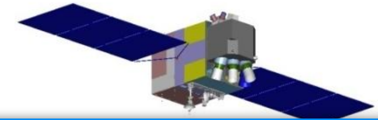

2 条带插补

Both Landsats 5 and Landsat 7 are still functioning. Landsats 5 has substantially exceeded its planned design lives

On May 31, 2003, the scan-line corrector (SLC) for the ETM+ sensor on board Landsat 7 failed permanently.

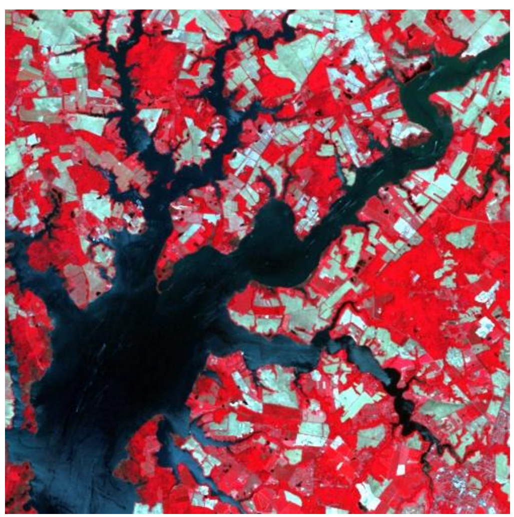

Landsat 5 TM

Landsat 7 ETM+

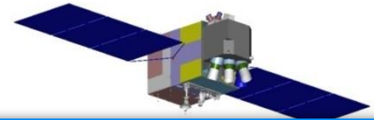

2 条带插补

Gap Filling: existing methods

- linear histogram-matching method (*USGS/NASA, 2004*): have **difficulty with heterogeneous** landscapes
- multi-scale segmentation approach (*Maxwell et al., 2007*): **lower accuracy at the pixel level**, especially for the narrow or small objects
- Geo-statistics based methods (*Zhang, et al., 2007; Pringle, et al., 2009*), using kriging or co-kriging techniques: predict the reflectance **not well at the pixel-level and very computationally intensive**

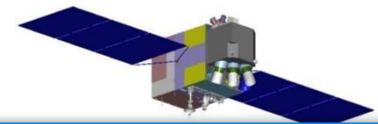

2 条带插补

☐ For Our Method

- Assumption:
- **Neighboring pixels** in close proximity to SLC-off gaps **share similar spectral characteristics and temporal patterns of changes with the missing pixels**, if they belong to the same land cover type.
- It is logical to make use of the information of the same-class neighboring pixels to restore spectral values of missing pixels Called as the **Neighborhood Similar Pixel Interpolator (NSPI)**
- Two data sources that can be used :
- (1) TM image or SLC-on ETM+ image, and (2) SLC-off images

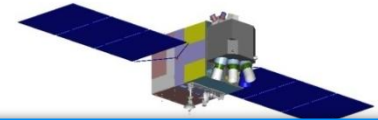

2 条带插补

- Using a single TM or SLC-on ETM+ image

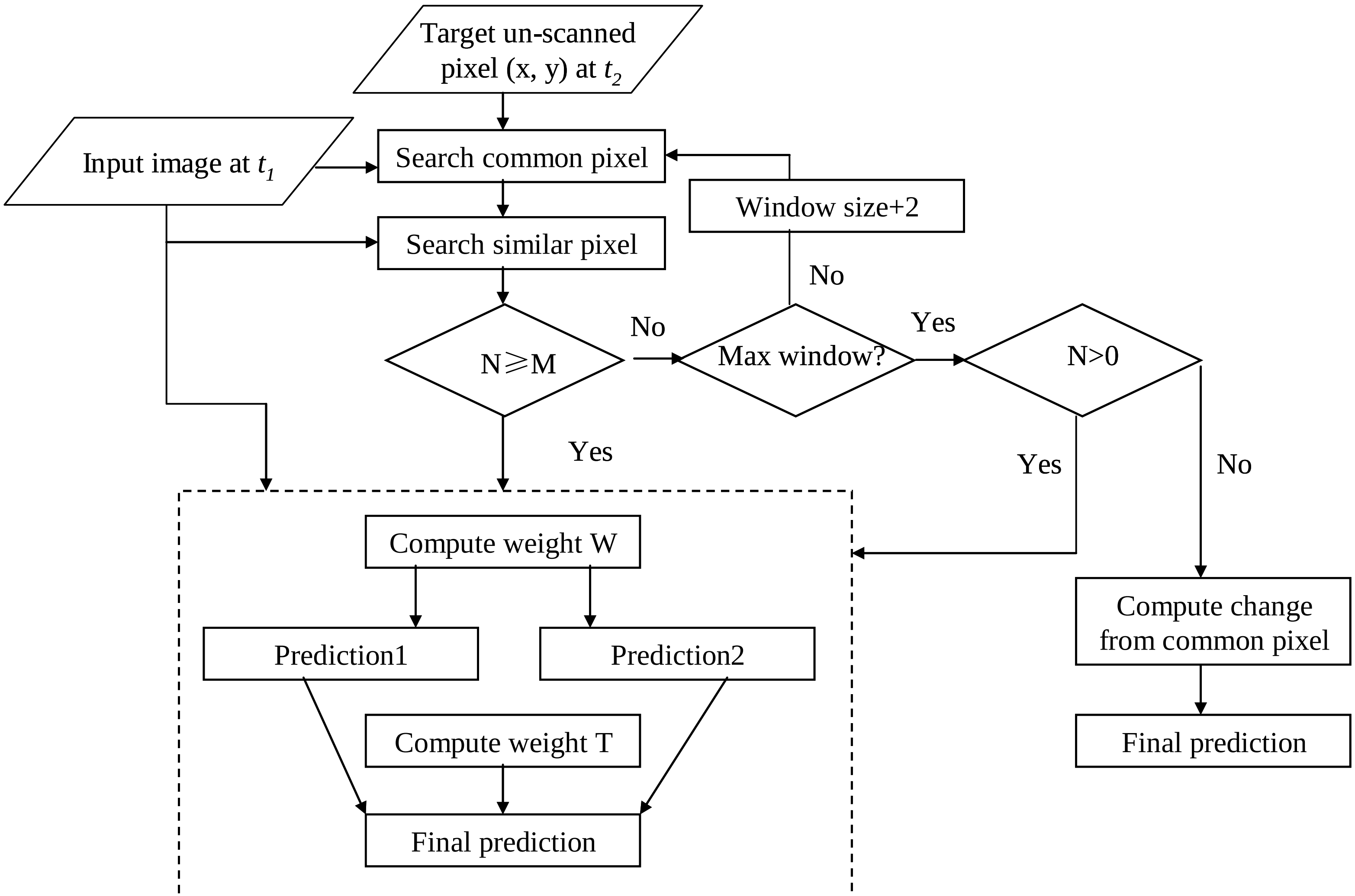

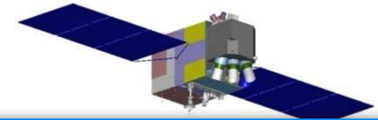

2 条带插补

Step 1 Step 2 Step 3 Step 4

Selection of neighboring similar pixels

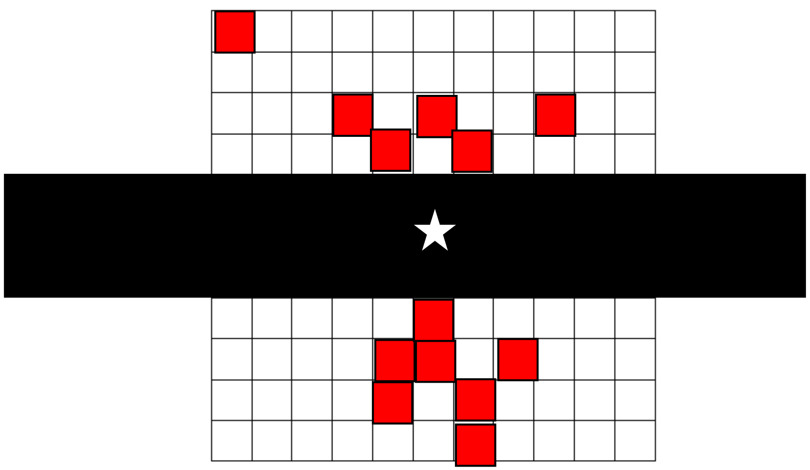

☆ Target pixel ■ Similar pixel

□ Common pixel

■ Gap in target image

$$RMSD_i = \sqrt{\frac{\sum_{b=1}^{n} (L(x_i, y_i, t_1, b) - L(x, y, t_1, b))^2}{n}}$$

Threshold:

$$RMSD_i \le [\sum_{b=1}^{n} \sigma(b) \times 2 / m] / n$$

initial moving window size:

$$IWS = \lfloor (\sqrt{M} + 1) / 2 \rfloor * 2 + 1$$

M is the required sample size, maximum window size 17×17

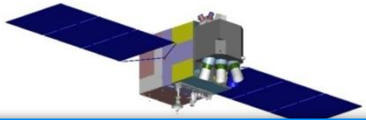

2 条带插补

Step 1 Step 2 Step 3 Step 4

Calculation of weight for similar pixels

This is determined by the location of the similar pixel and the spectral similarity between the similar pixel and target pixel

$$D_j = \sqrt{(x_j - x)^2 + (y_j - y)^2}$$

$$CD_j = RMSD_j \times D_j$$

$$W_j = (1/CD_j)/\sum_{j=1}^{N}(1/CD_j)$$

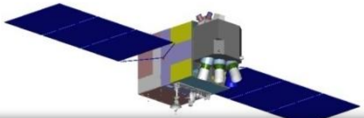

2

条带插补

Step 1 Step 2 **Step 3** Step 4

Calculation of value of the target pixel

two methods to predict the value of the target pixel :

- **first prediction**: the weighted average of all the similar pixels:

$$L_1(x, y, t_2, b) = \sum_{j=1}^{N} W_j \times L(x_j, y_j, t_2, b)$$

- **Second prediction**: the sum of value at t1 and the change from t1 to t2

$$L_2(x, y, t_2, b) = L(x, y, t_1, b) + \sum_{j=1}^{N} W_j \times (L(x_j, y_j, t_2, b) - L(x_j, y_j, t_1, b))$$

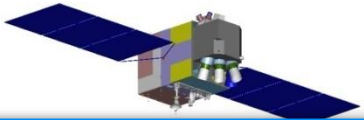

2 条带插补

Step 1 Step 2 Step 3 **Step 4**

Combine the two predictions with weights:

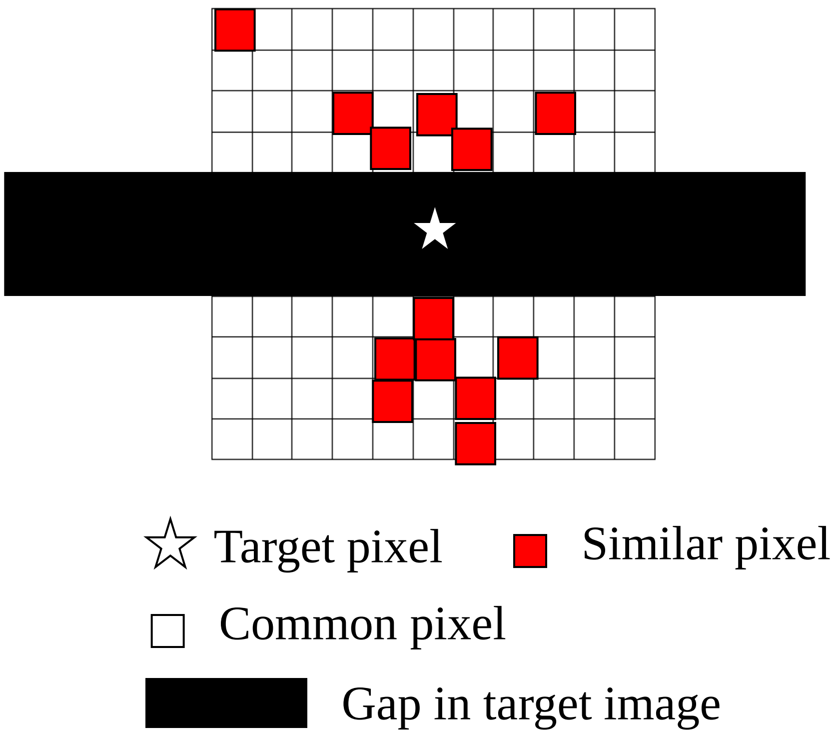

$$R_1 = \frac{1}{N}\sum_{j=1}^{N}\sqrt{[\sum_{b=1}^{n}(L(x_j, y_j, t_1, b) - L(x, y, t_1, b))^2]/n}$$

$$R_2 = \frac{1}{N}\sum_{j=1}^{N}\sqrt{[\sum_{b=1}^{n}(L(x_j, y_j, t_1, b) - L(x_j, y_j, t_2, b))^2]/n}$$

$$T_i = (1/R_i)/(1/R_1 + 1/R_2)$$

$$L(x, y, t_2, b) = T_1 \times L_1(x, y, t_2, b) + T_2 \times L_2(x, y, t_2, b)$$

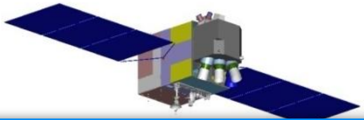

2 条带插补

All input images are sorted based upon acquisition date.

the maximum window size is increased from 17 to 31

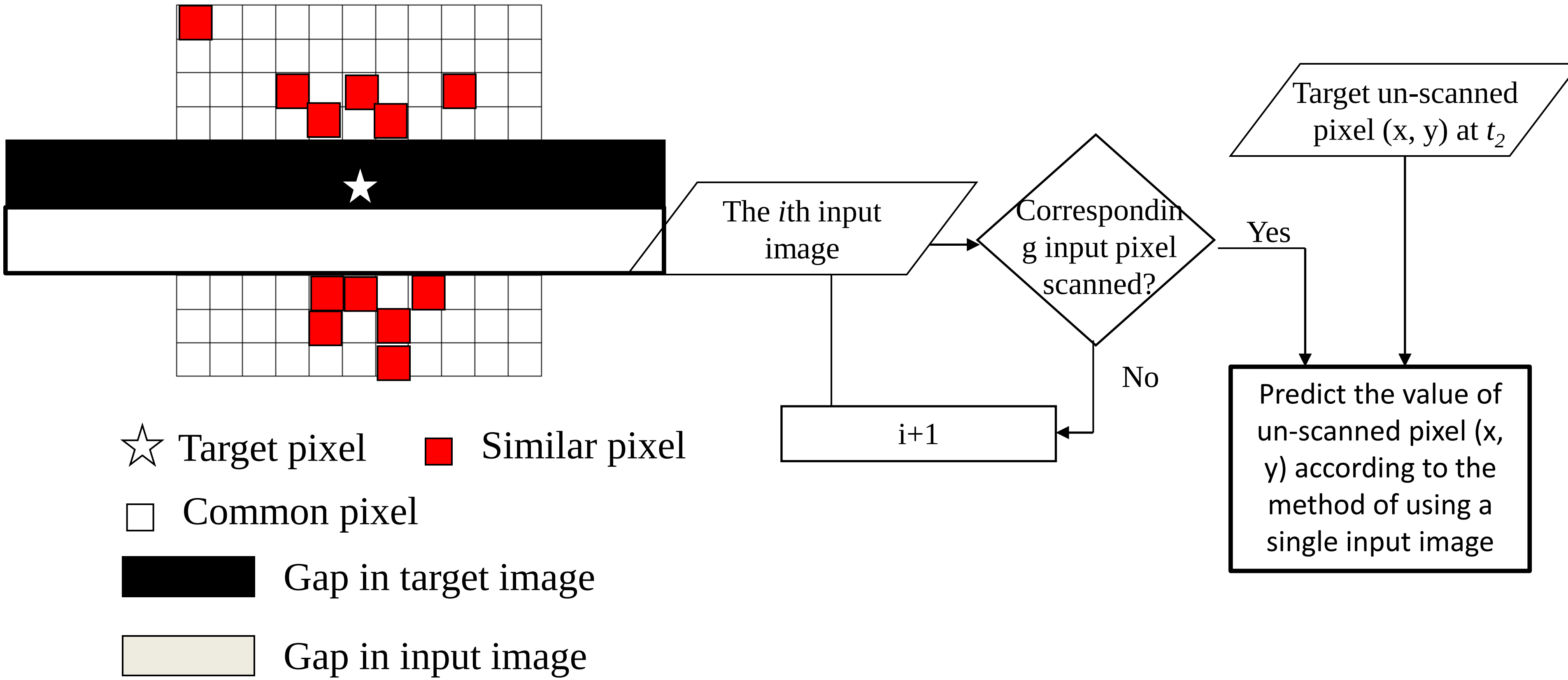

2 条带插补

Test results

Simulated SLC-off images : test single input image

TM 5/25/2008

TM 6/10/2008

Simulated 6/10/2008

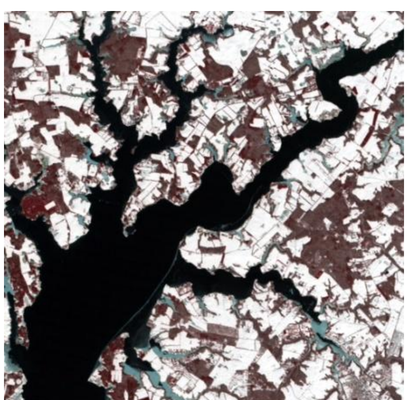

TM 2/8/2010

TM 4/29/2010

Simulated 4/29/2010

2 条带插补

Optimization of sample size M:

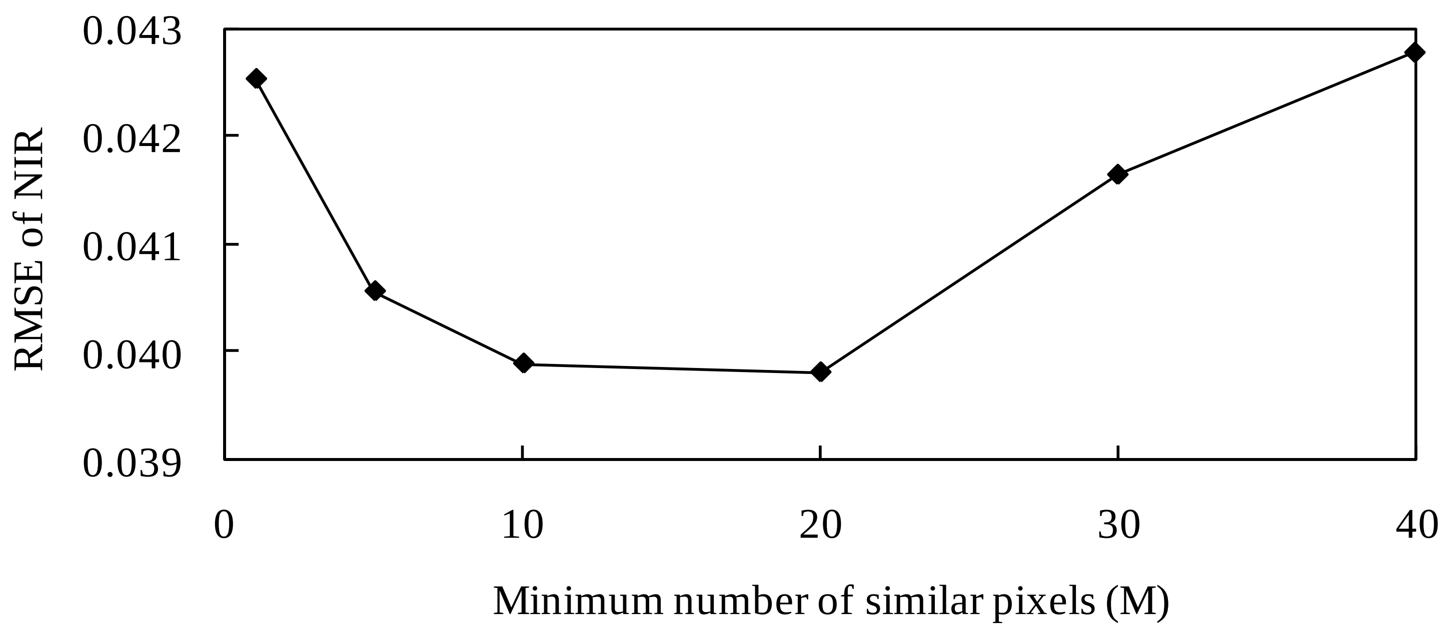

recommend 20 as an appropriate value of *M*

2 条带插补

Filled results of Simulated SLC-off image

6/10/2008 filled by USGS

6/10/2008 filled by NSPI

True image

4/29/2010 filled by USGS

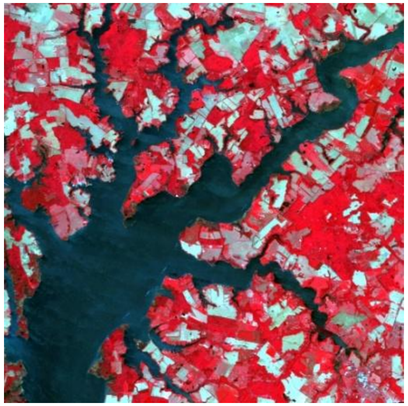

4/29/2010 filled by NSPI

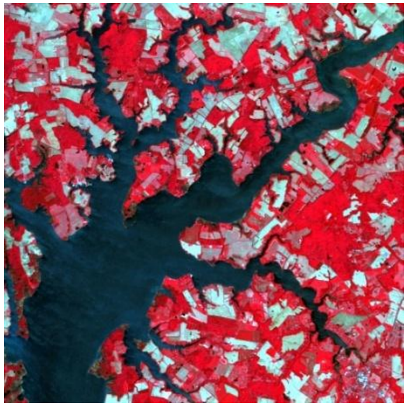

True image

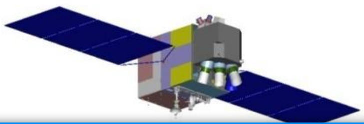

2 条带插补

Scatter plot of filled image v.s. true image

6/10/2008

4/29/2010

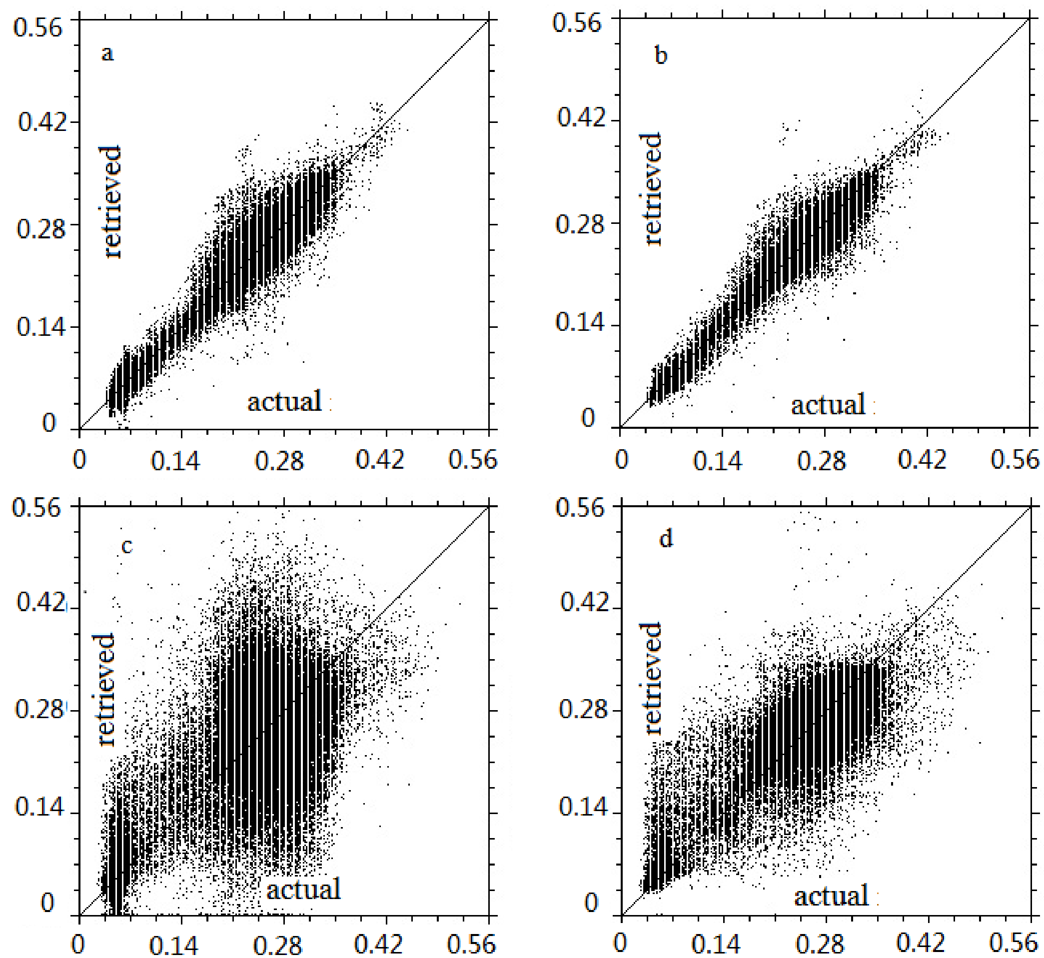

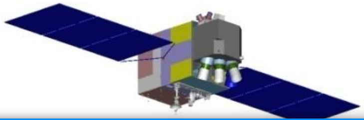

2 条带插补

Test results

Simulated SLC-off images : test single input image

The accuracy of filled results of Fig.5 c and f using a single input image

Band	Method	Filled result of Fig.5 c			Filled result of Fig.5 f		
		RMSE	AAD	AD	RMSE	AAD	AD
Green	Histogram Matching	0.0070	0.0043	0.0000	0.3696	0.1791	-0.1600
	NSPI	0.0052	0.0032	0.0000	0.0121	0.0068	-0.0007
Red	Histogram Matching	0.0107	0.0061	0.0000	0.4006	0.1960	-0.1817
	NSPI	0.0079	0.0045	0.0000	0.0173	0.0097	-0.0008
NIR	Histogram Matching	0.0195	0.0114	-0.0002	0.0960	0.0520	-0.0036
	NSPI	0.0153	0.0093	0.0001	0.0398	0.0244	0.0005

2 条带插补

Test results

Simulated SLC-off images : test single input image

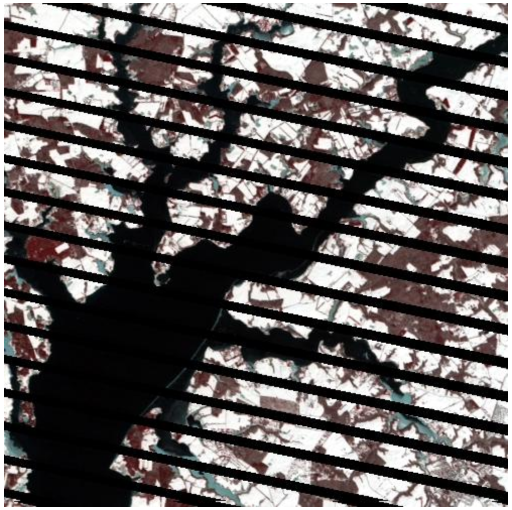

Simulated 2/8/2010

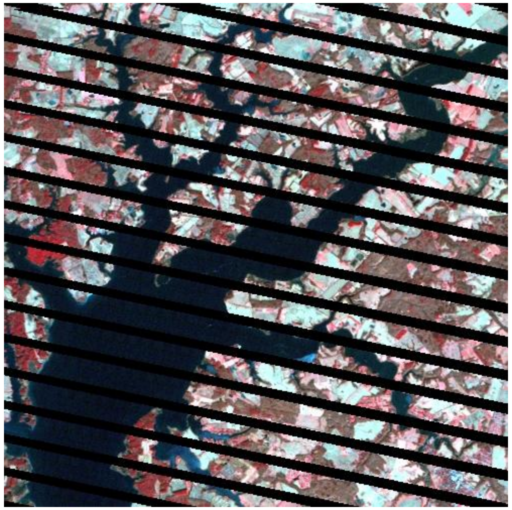

Simulated 1/23/2010

Simulated 4/29/2010

2 条带插补

Test results

Simulated SLC-off images : test single input image

4/29/2010

USGS NSPI

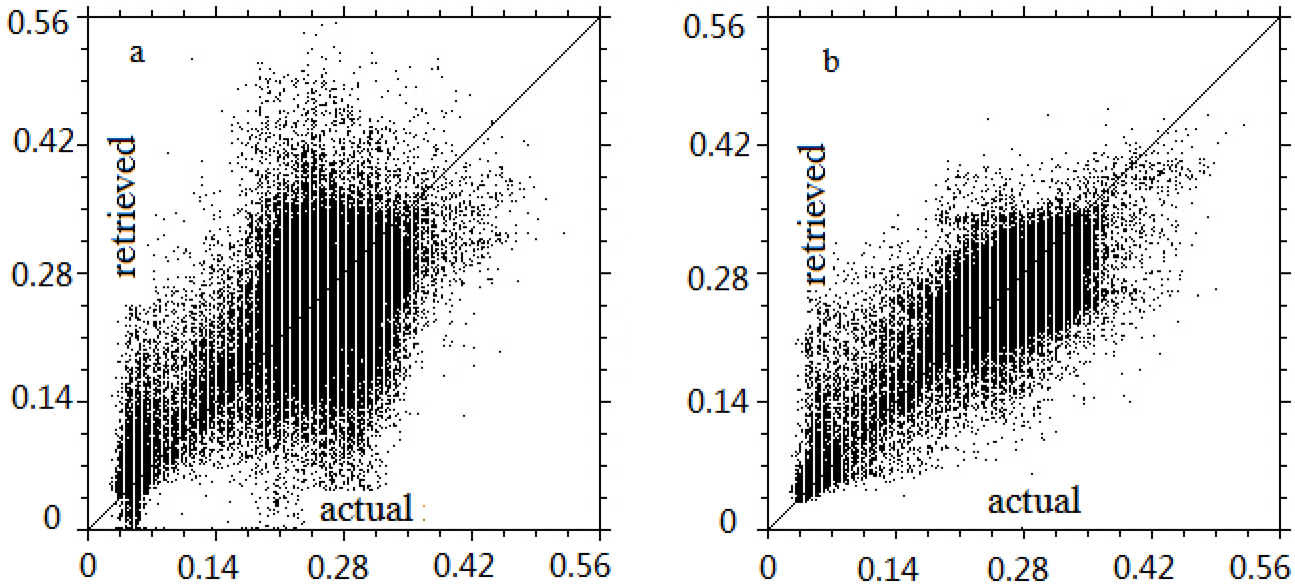

2 条带插补

Test results: True SLC-off images

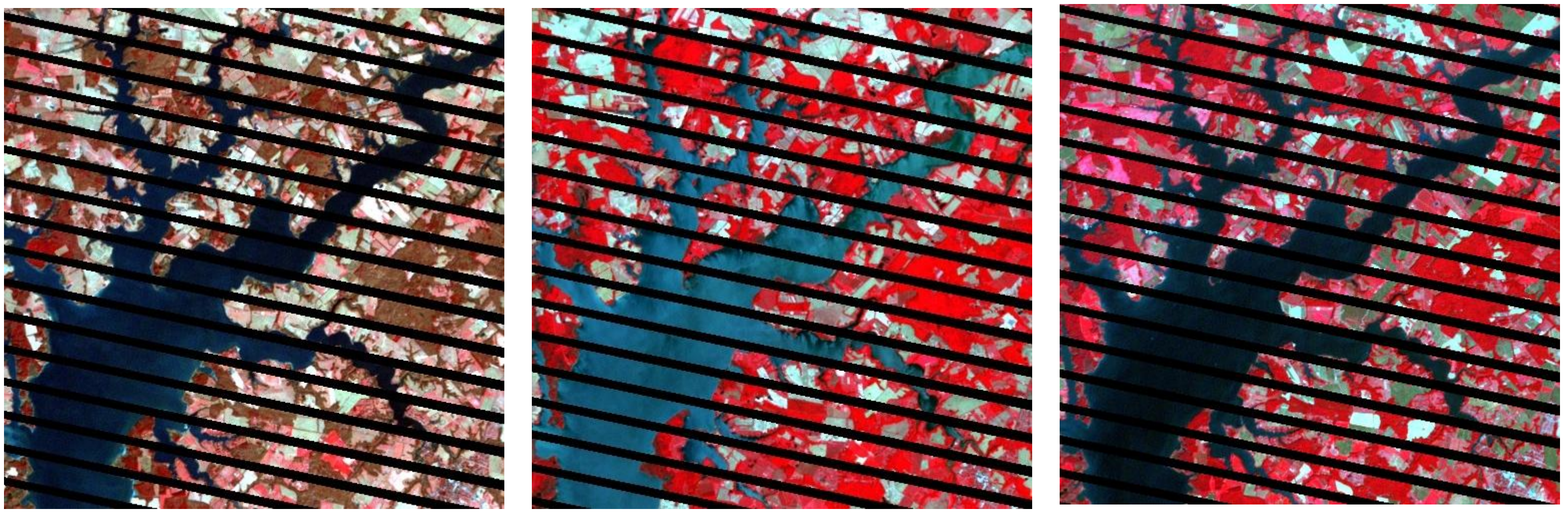

(a) acquired at February 11, 2008; (b) acquired at June 8, 2008; (c) acquired at September 22, 2008

2 条带插补

Test results: True SLC-off images

Using single input

USGS

NSPI

Using multiple inputs

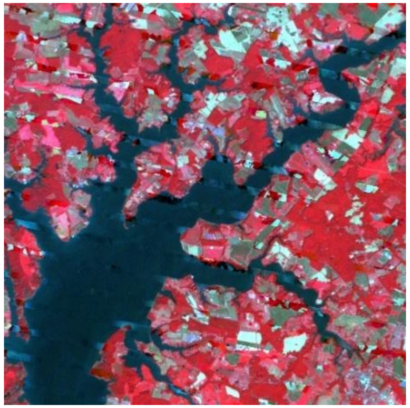

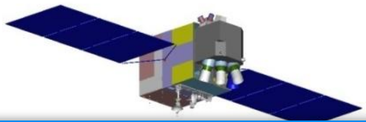

2 条带插补

Test results: True SLC-off images

- Land cover classification accuracy assessment (James E. Vogelmann, USGS)
- For gap areas, overall classification accuracies were 90.8% and 92.7% for gap-filled versus reference data sets, respectively

Class	Reference Totals	Classified Totals	Number Correct	Producer's Accuracy	User's Accuracy
Water	47 **47**	45 **43**	45 **43**	95.7% **91.5%**	100.0% **100.0%**
Ag and Grass	67 **67**	85 **75**	67 **66**	100.0% **98.5%**	78.8% **88.0%**
Forest	74 **74**	61 **70**	61 **68**	82.4% **91.9%**	100.0% **97.1%**
Urban	15 **15**	12 **14**	12 **12**	73.3% **80.0%**	91.7% **85.7%**
Wetlands	3 **3**	3 **4**	3 **2**	100.0% **66.7%**	100.0% **50.0%**

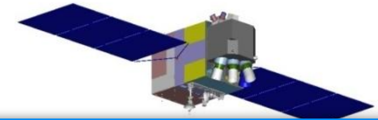

2 条带插补

Compared with the existing methods, the NSPI can restore the value of un-scanned pixels very accurately, especially for heterogeneous landscapes and when there is a longer time interval between the input image and target image;

The **major improvements** of NSPI : better use of useful and relevant information of the scanned pixels; ensure the spatial continuity of the filled results .

Potential limitations: require the availability of one or more ancillary TM or ETM+ image(s), unclear how much changing land cover will impact final results

3 厚云去除

- 云污染是常见现象，影响地表特征的提取；
- 主要2类：薄云，厚云

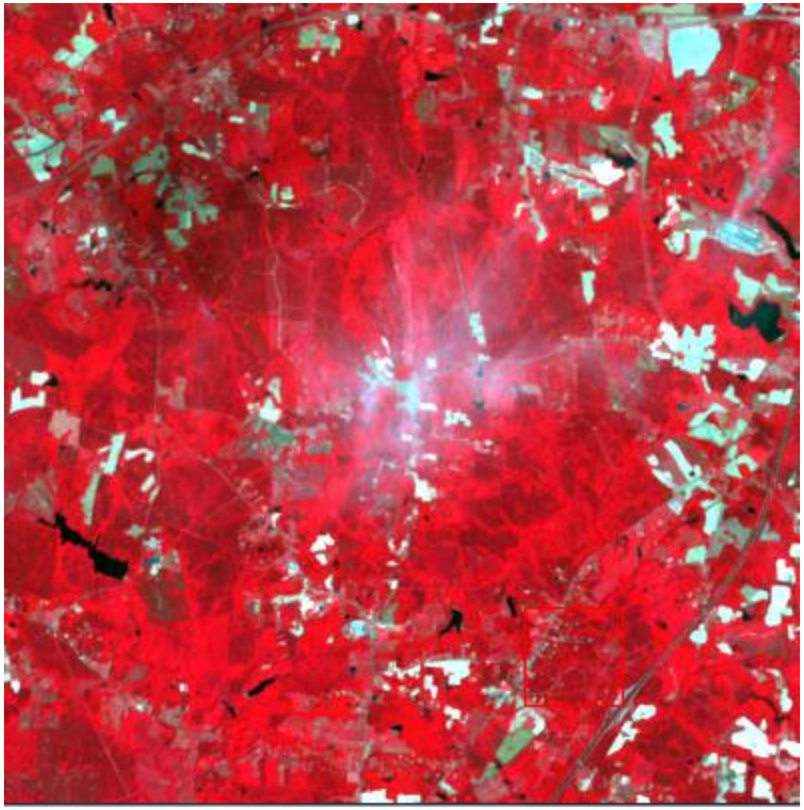

薄云

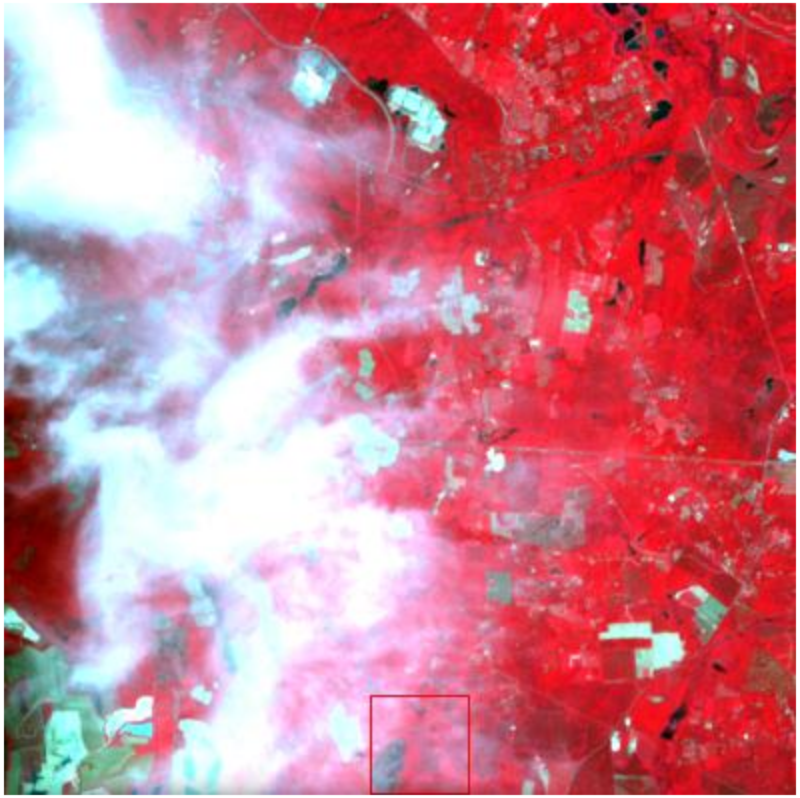

厚云

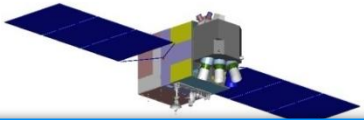

3 厚云去除

常用的云处理方法：

1）薄云处理：恢复云下弱信息，比如缨帽变换，FFT，数据融合，直方图匹配等方法；

2）厚云处理：最常见的为替换法。其缺点为：反演反射率的误差大，视觉上有斑块状。

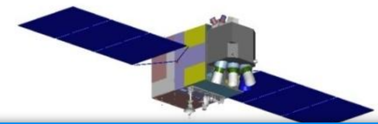

3 厚云去除

常用的云处理方法：

1）薄云处理：恢复云下弱信息，比如缨帽变换，FFT，

2）厚云处理：最 其缺点为：反演反射

率的误差大，视觉上有斑块状。

发展一种**基于多源遥感数据**的厚云处理方法，得到较为准确的反射率产品。

3 厚云去除

为检验方法，在Landsat影像上模拟厚云：

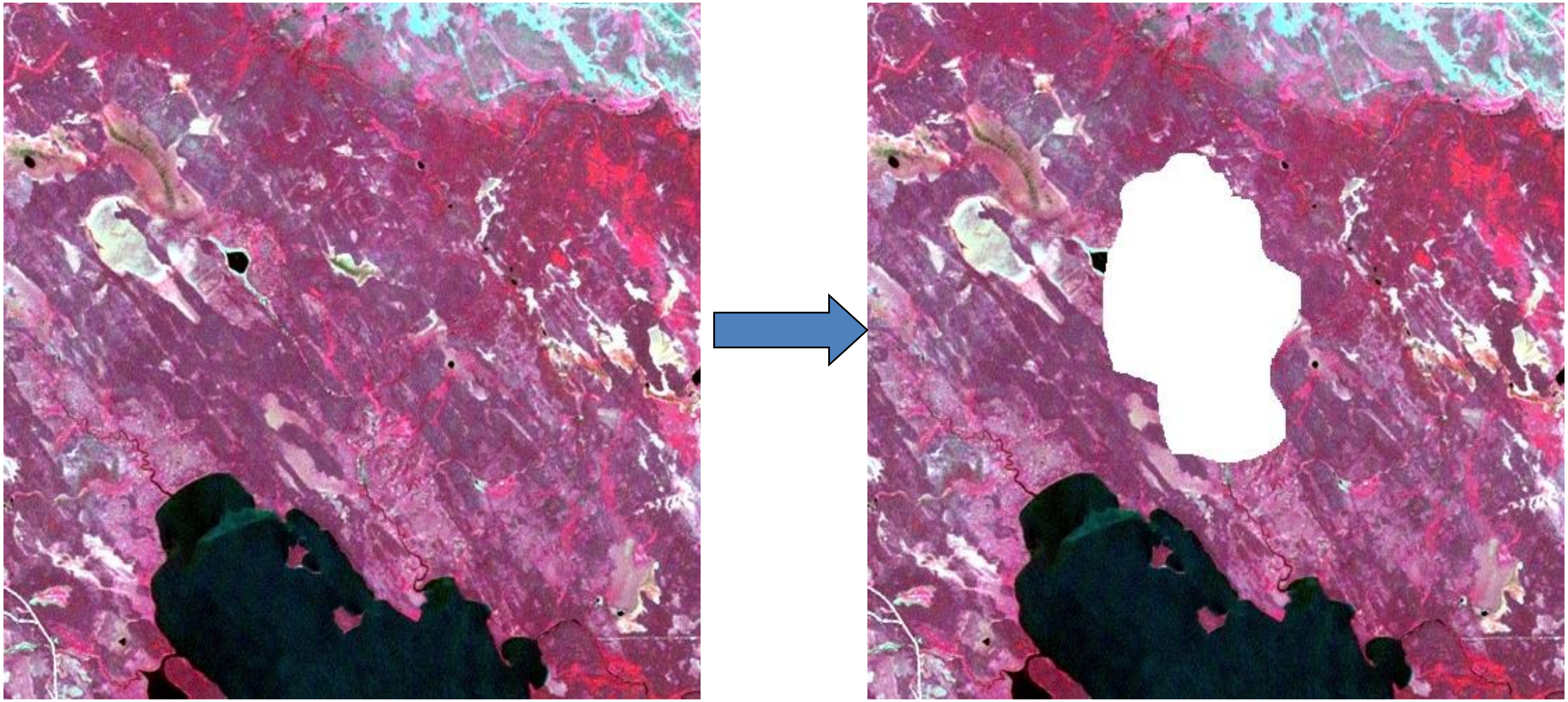

2001-7-11 landsat

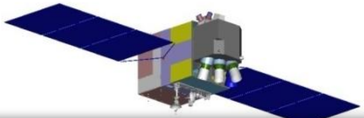

3 厚云去除

- 辅助数据：如果仅有一幅时间接近的清晰Landsat影像可用

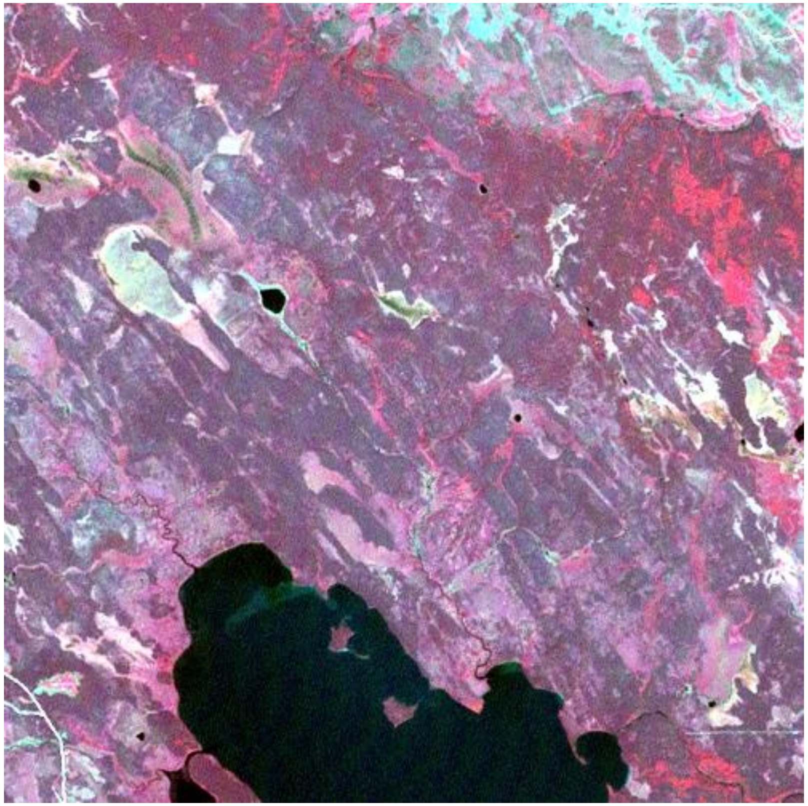

2001-8-12 landsat

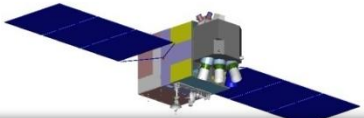

3 厚云去除

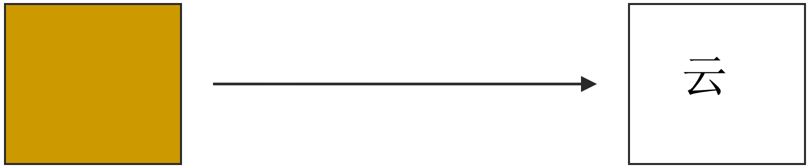

t1 t2

$$L(x, y, t_2) = L(x, y, t_1) + \Delta L(x, y)$$

假设空间临近的同类地物的变化量相同：

$\Delta L(x, y)$ 可以由云周围的非云像元提供。

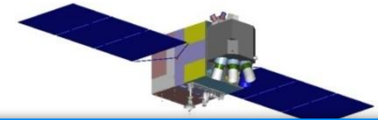

3 厚云去除

流程图

步骤1

步骤2

步骤3

步骤4

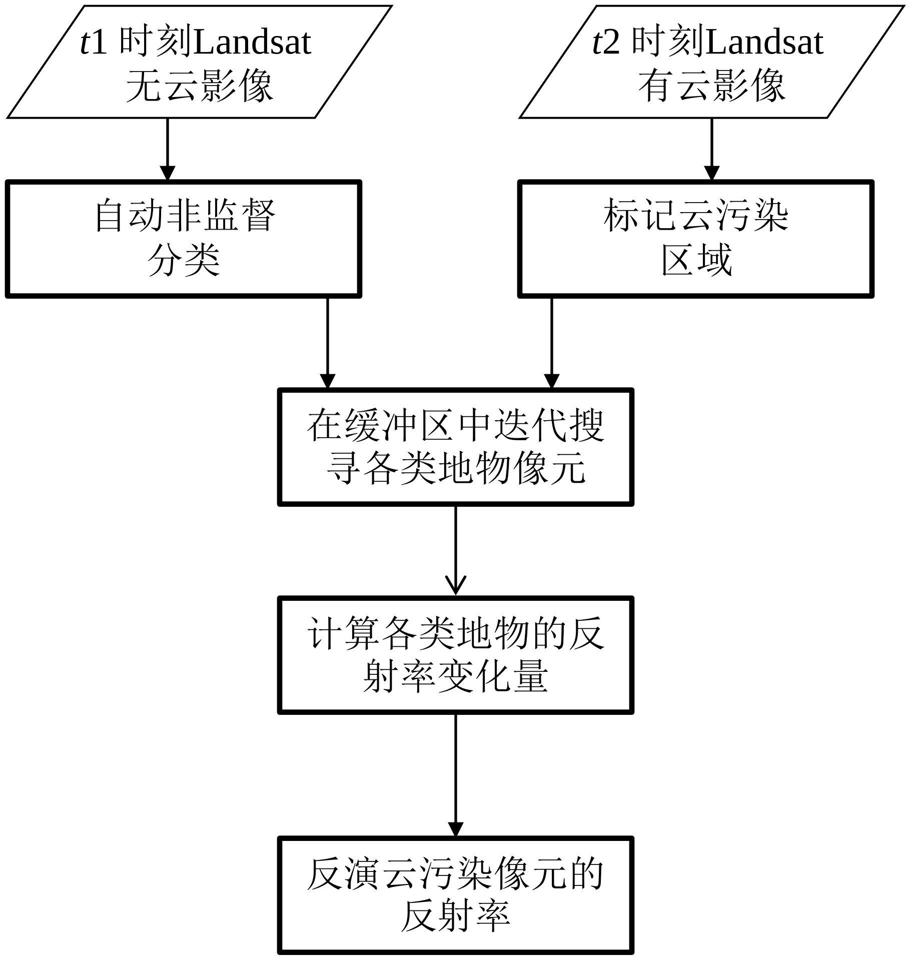

3 厚云去除

Step 1 | Step 2 | Step 3 | Step 4

自动分类结果

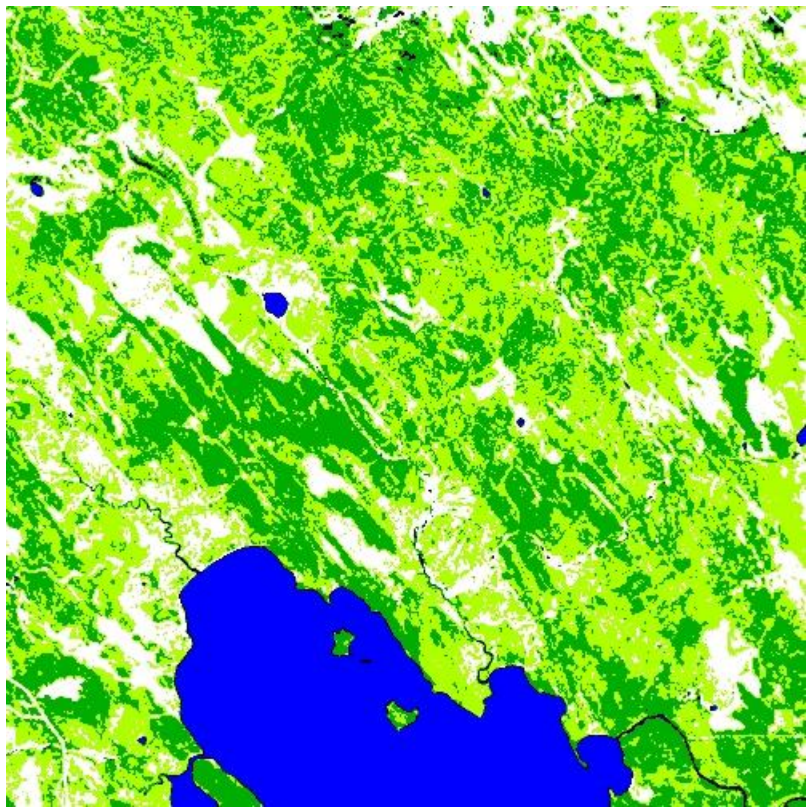

dense vegetation
thin vegetation
high-reflectance bareness
low-reflectance bareness
water

3

厚云去除

Step 1 Step 2 Step 3 Step 4

缓冲区迭代搜寻各类地物

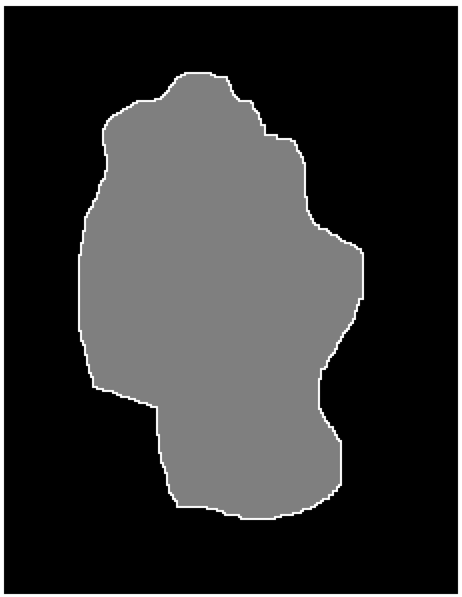

1）在云周围生成1个像元宽度的缓冲区，在该缓冲区中搜寻各类地物，并标记；

2）如果所有地物类型的像元都找到（而且像元数目大于某一阈值），则搜寻停止；

3）如果还有地物类别没有找到，则生成2个像元宽的缓冲区，继续搜寻，直到找到所有地物。

对于本例，搜寻到第5层缓冲区时找到所有5类地物的像元（大于50个）。

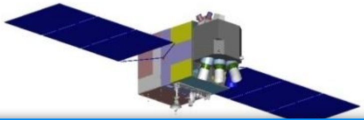

3 厚云去除

Step 1 Step 2 Step 3 Step 4

计算各类地物的反射率变化量

$$\Delta L_i = \frac{\sum_{j=1}^{m} [L(x_j, y_j, t_2) - L(x_j, y_j, t_1)]}{m}$$

其中，j是指上一步骤中搜寻到的i类地物m个像元中的第j个像元。

各类地物各波段的变化量：值/10000

band	class 1	class 2	class 3	class 4	class 5
green	51.93	65.85	57.08	41.11	62.29
red	26.55	75.02	35.05	33.08	53.37
NIR	143.36	52.37	154.63	42.39	116.56

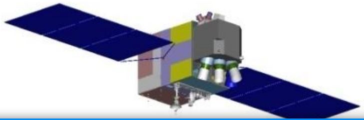

3 厚云去除

Step 1 Step 2 Step 3 **Step 4**

反演云像元的反射率

- 1）云边缘的区域：即可直接由t2时刻相邻同类地物的反射率得到L1(x,y,t2)，也可由t1时刻的反射率加上变化量得到L2(x,y,t2)，用权重将二者结合得到反演结果：

$$w_1 = \frac{S1}{S1+S2} \qquad w_2 = \frac{S2}{S1+S2}$$

其中，S1,S2分别表示在目标像元为中心17*17窗口内，和目标像元同类的地物无云区域面积和被云污染的面积。

$$L(x,y,t_2) = \mathrm{w}_1 \times L_1(x,y,t_2) + \mathrm{w}_2 \times L_2(x,y,t_2)$$

- 2）云中区域：由t1时刻的反射率加上步骤3得到的变化量得到

$$L(x,y,t_2) = L(x,y,t_1) + \Delta L_k$$

3 厚云去除

Results

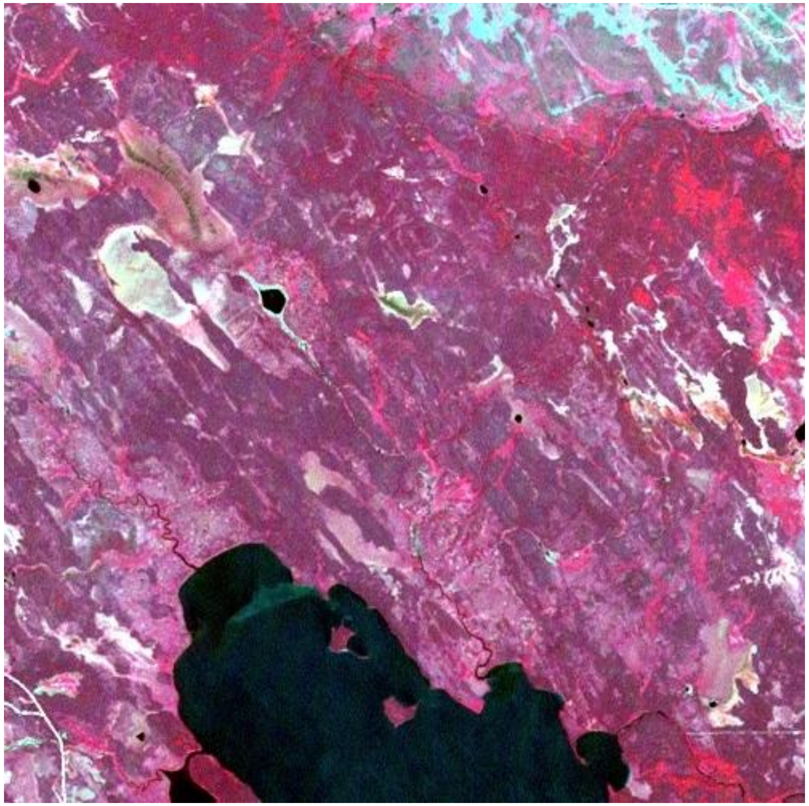

True image

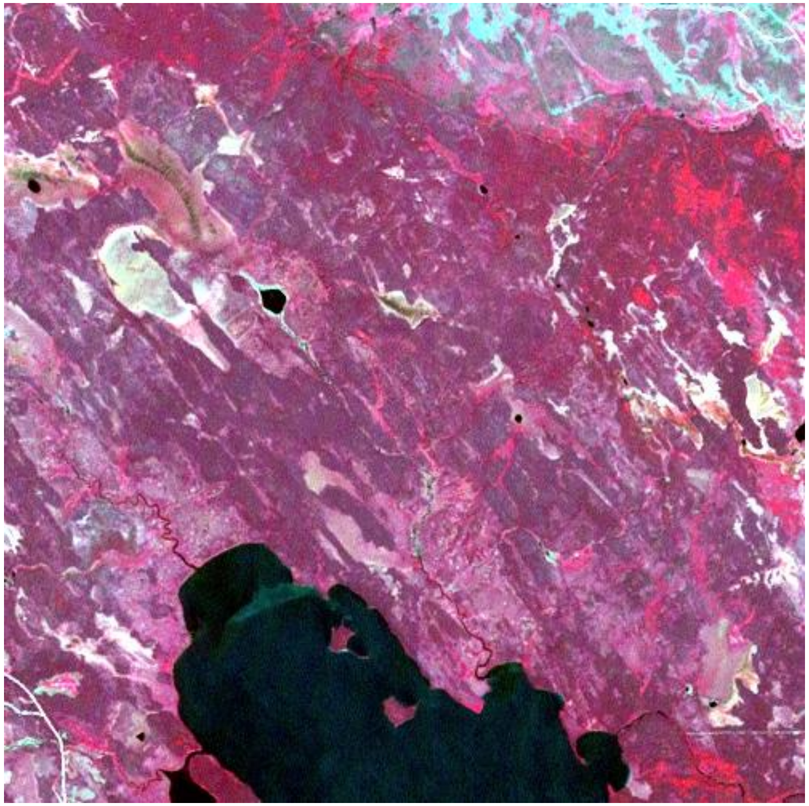

Retrieved image
Use 8/12 TM

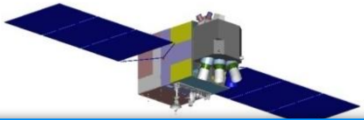

3 厚云去除

Results

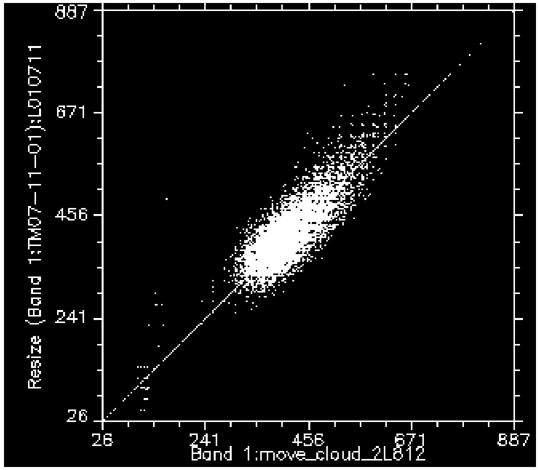

Green band

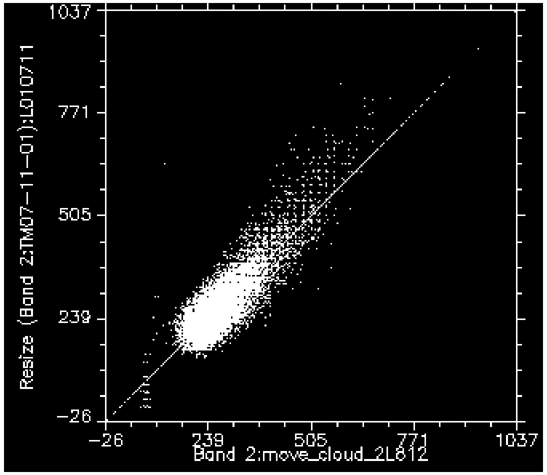

Red band

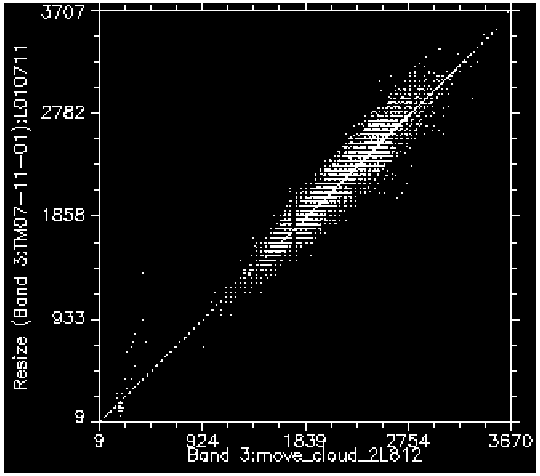

NIR band

	Average Absolute Difference (AAD)		Average Difference (AD)	
Band	2001/8/12	retrived	2001/8/12	retrieved
green	0.0059	0.0024	0.0058	0.0002
red	0.0041	0.0029	0.0035	-0.0001
NIR	0.0155	0.0061	0.0150	0.0011

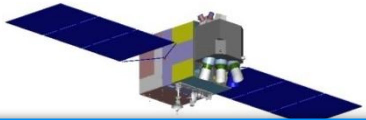

3 厚云去除

发展的新方法能较为精确地去除影像中的厚云污染，反演的的反射率误差很小，而且云处理后的影像视觉效果很好，没有斑块效果；

该方法自动，简单快捷，可以运用于海量遥感数据云处理。

4 山体阴影信息恢复

Mountainous shadows occur when objects totally or partially occlude **direct light** from a source of illumination, cause great difficulty in **land cover interpretation and classification**.

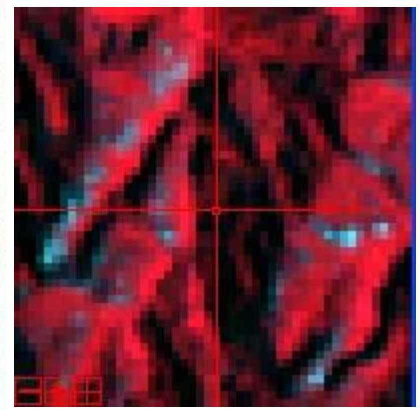

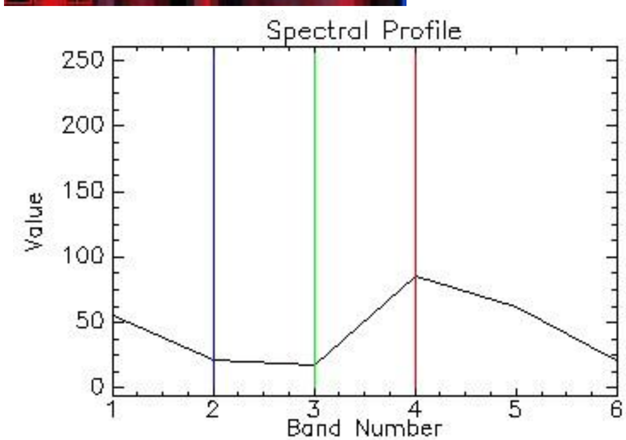

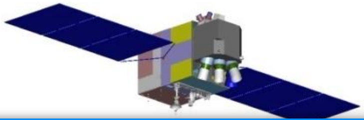

4 山体阴影信息恢复

Topographic correction methods can partly alleviate the impact of shadows. But they have tow limitations:

1) little effect on areas with very low incidence angles and those completely with no direct solar illumination (cast shadow);
2) Complete DEM data with adequate spatial resolution and elevation accuracy.

Our research is to restore shadow spectral information:

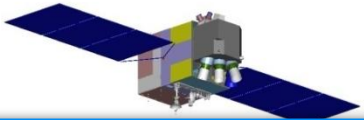

4 山体阴影信息恢复

Step 1 | ep | Step | Step | Step 5

Shadow Detection

TC transformation→Brightness band

↓

Brightness of all segmented objects-
average brightness of all pixels within the object

↓

Automatic thresholding method

↓

Brightness<threshold → shadow object
Brightness>threshold → non-shadow object

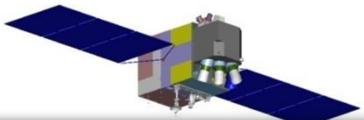

4 山体阴影信息恢复

Step | Step 2 | ep | Step | Step 5

Image Segmentation: Shadows in mountainous terrain often fall within a certain range of shapes and sizes:

- Detect shadow at object scale rather than at pixel scale;
- Image segmentation.

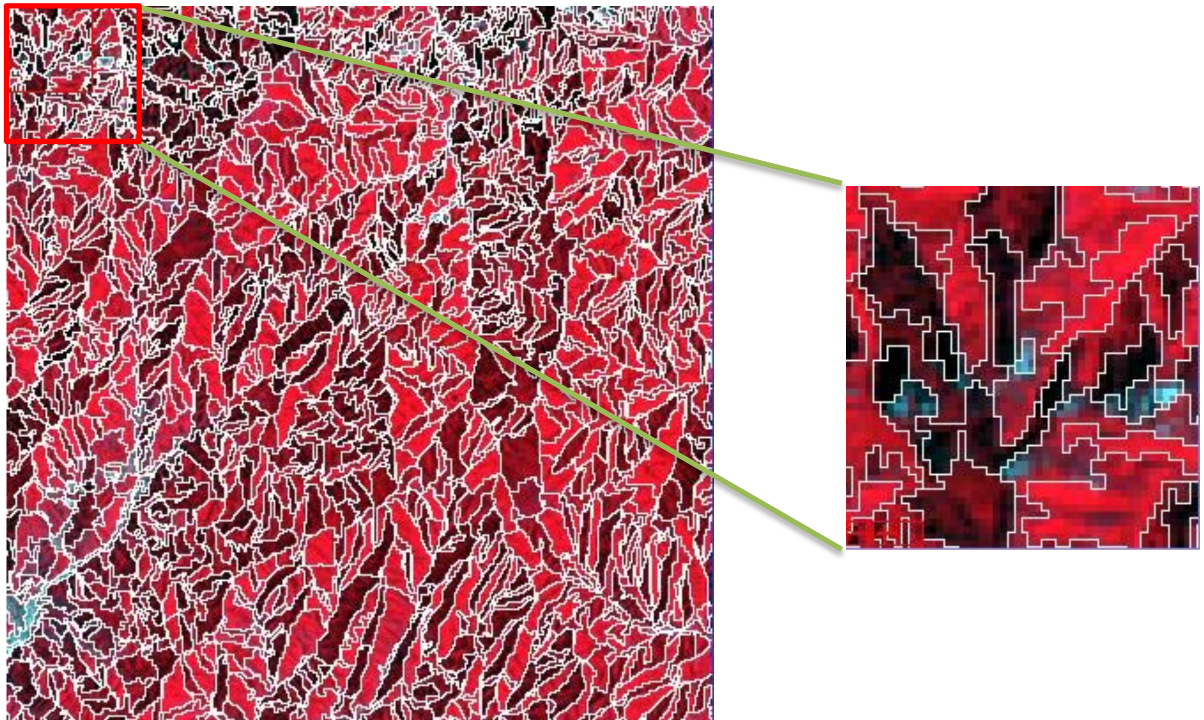

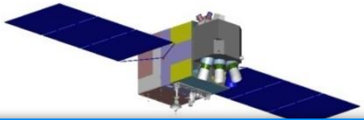

4 山体阴影信息恢复

Step Step **Step 3** tep Step 5

Shadow Detection

- Validation

Detected shadow

Hillshade derived from DEM

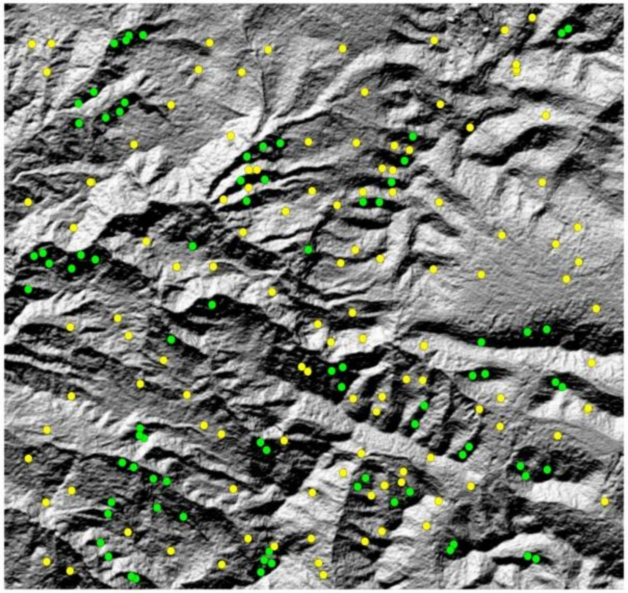

Omission error: 2.5%; Commission error: 8.3%; Overall accuracy: 90%

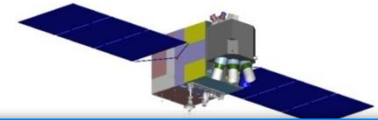

4 山体阴影信息恢复

Step Step Step **Step 4** tep 5

Search for Non-shaded Similar Pixels

- Continuum Removal (CR)
  - to separate a spectrum into two parts:
    - brightness information (CI)
    - spectral shape information (CR)
    - CR: divide original spectrum by continuum line

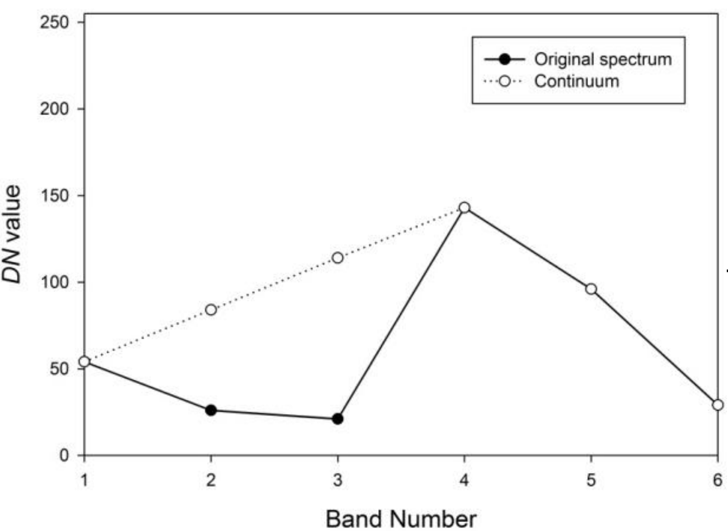

$$CR_\lambda = \frac{OI_\lambda}{CI_\lambda}$$

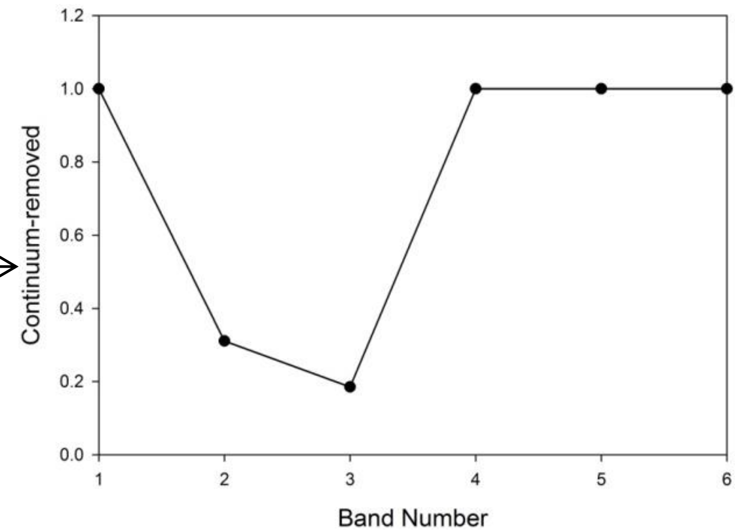

Search for Non-shaded Similar Pixels

- Create a buffer with width of two pixels around a shadow object;
- For a specific target pixel, search for *N* spectrally nearest pixels within the buffer area as the non-shaded similar pixels;
- If the number of found similar pixels < *N*, repeatedly expand the buffer by two pixels to continue researching, until *N* is met.

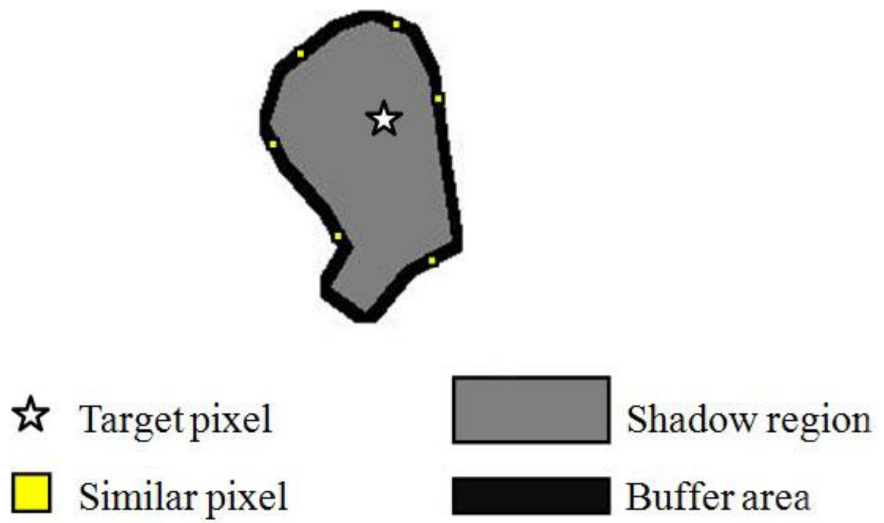

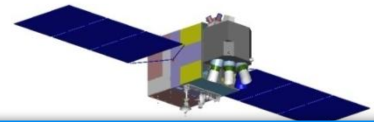

4 山体阴影信息恢复

Step Step Step **Step 4** tep 5

Search for Non-shaded Similar Pixels

– Similarity Condition:

$$RMSD_i = \sqrt{\frac{\sum_{b=1}^{n}\left(CR(x_i, y_i, b) - CR(x, y, b)\right)^2}{n}}$$

$$RMSD_i \le \left[\sum_{b=1}^{n}\sigma(b)\times 2/m\right]/n \;\begin{cases}\text{Yes, similar pixel} \\ \text{No, not similar pixel}\end{cases}$$

- CR (x_i, y_i, b): CR value of ith non-shaded pixel located at (x_i, y_i) in band b;
- CR (x, y, b): same as CR (x_i, y_i, b) but for the target pixel;
- n: number of bands;
- σ(b): standard deviation of the CR value for the whole test image in band b;
- m: estimated number of land cover classes.

Shadow Information Restoration

- Combine the CR of the target shaded pixel and the CI of its non-shaded similar pixels:

$$OI_{re(b)} = CI_{wavg(b)} \times CR_{(b)}$$

  - $OI_{re(b)}$: restored *DN* value of the target shaded pixel at band(b);
  - $CR_{(b)}$: the continuum removed value of the target shaded pixel at band(b);
  - $CI_{wavg(b)}$: the weighted average continuum values of non-shaded similar pixels.

$$CI_{wavg(b)} = \sum_{j=1}^{N} W_j \times CI_{j(b)}$$

  - W_j: the contribution of similar pixel *j*. It is related to both the geographic distance between the similar pixel and the target pixel and the spectral similarity between them.

4 山体阴影信息恢复

Case study

- Study area: Shaanxi province, China, 109°1′24″ E, 33°57′22″ N
  - Forests dominate the mountainous areas in the southern part;
  - Crops, urban areas, and barren lands cover the northern part of the test area.
  - Landsat 5 TM image: acquired on June 30, 2009

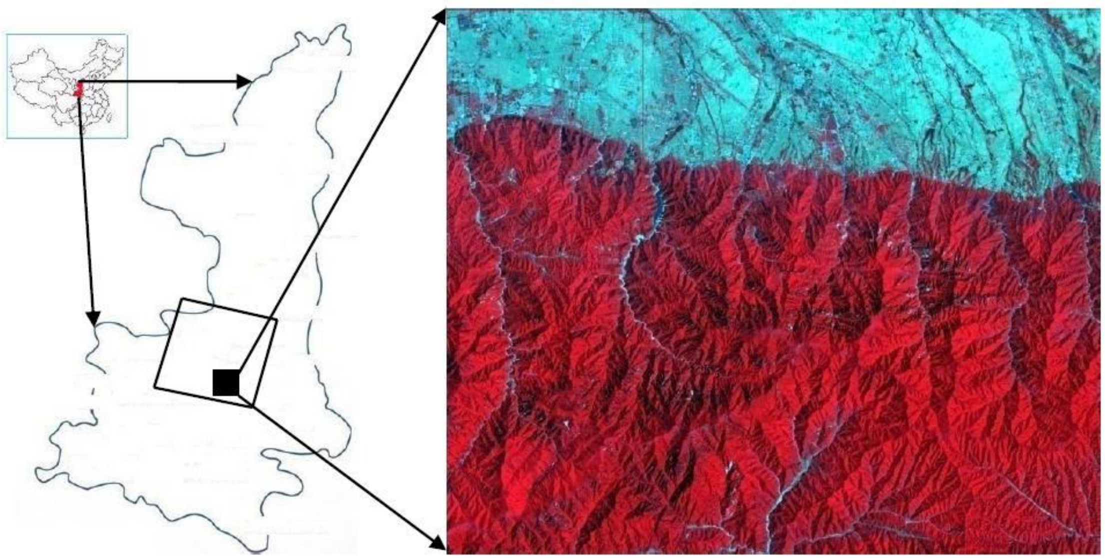

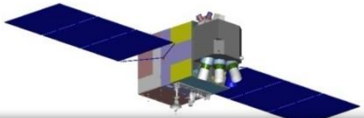

4 山体阴影信息恢复

Case study

CR method

Topographic correction
(DEM resolution:90m)

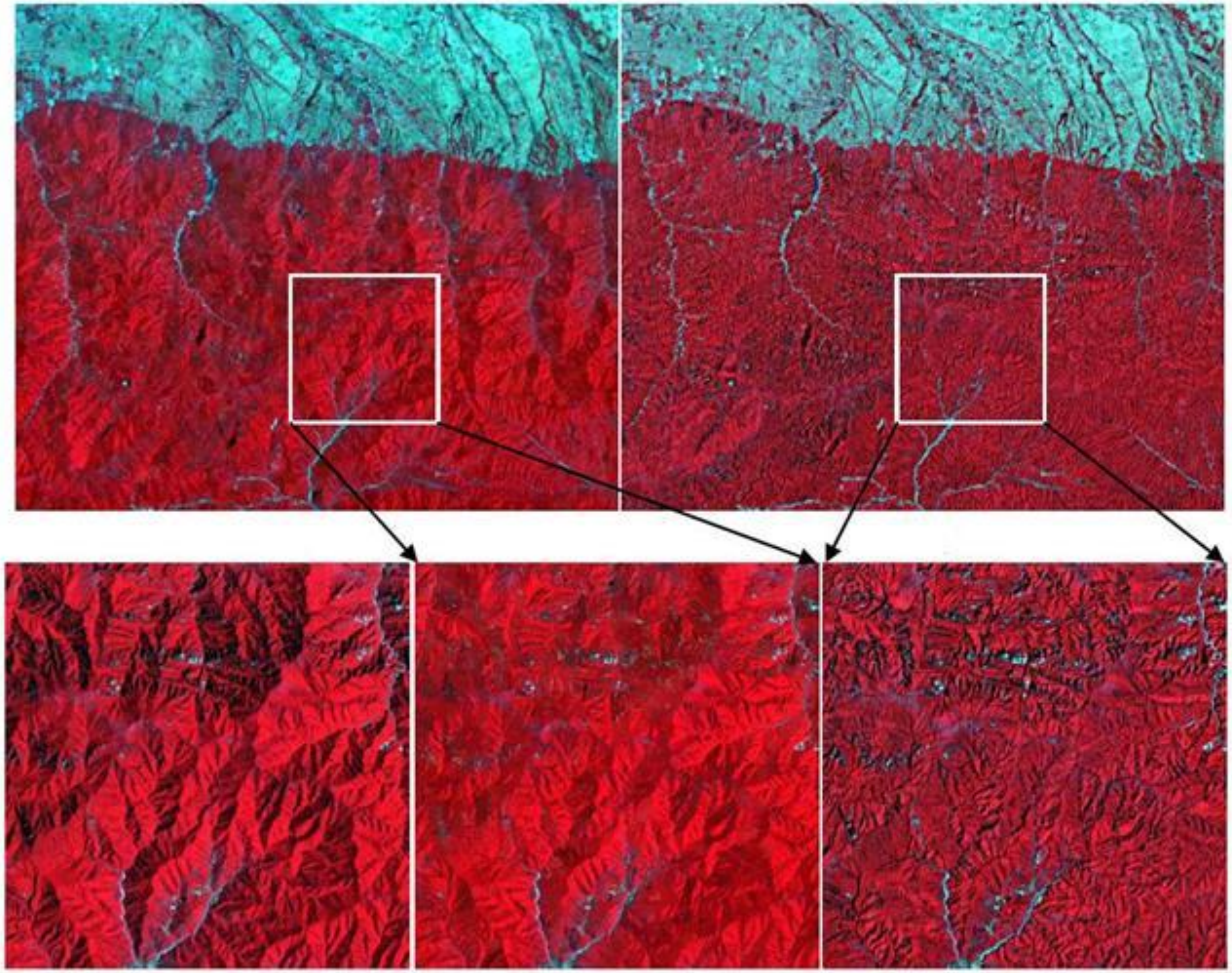

4 山体阴影信息恢复

Case study

- Spectral comparison before and after shadow restoration

*The former two curves are presented in TOA reflectance;
the latter two are presented in surface reflectance

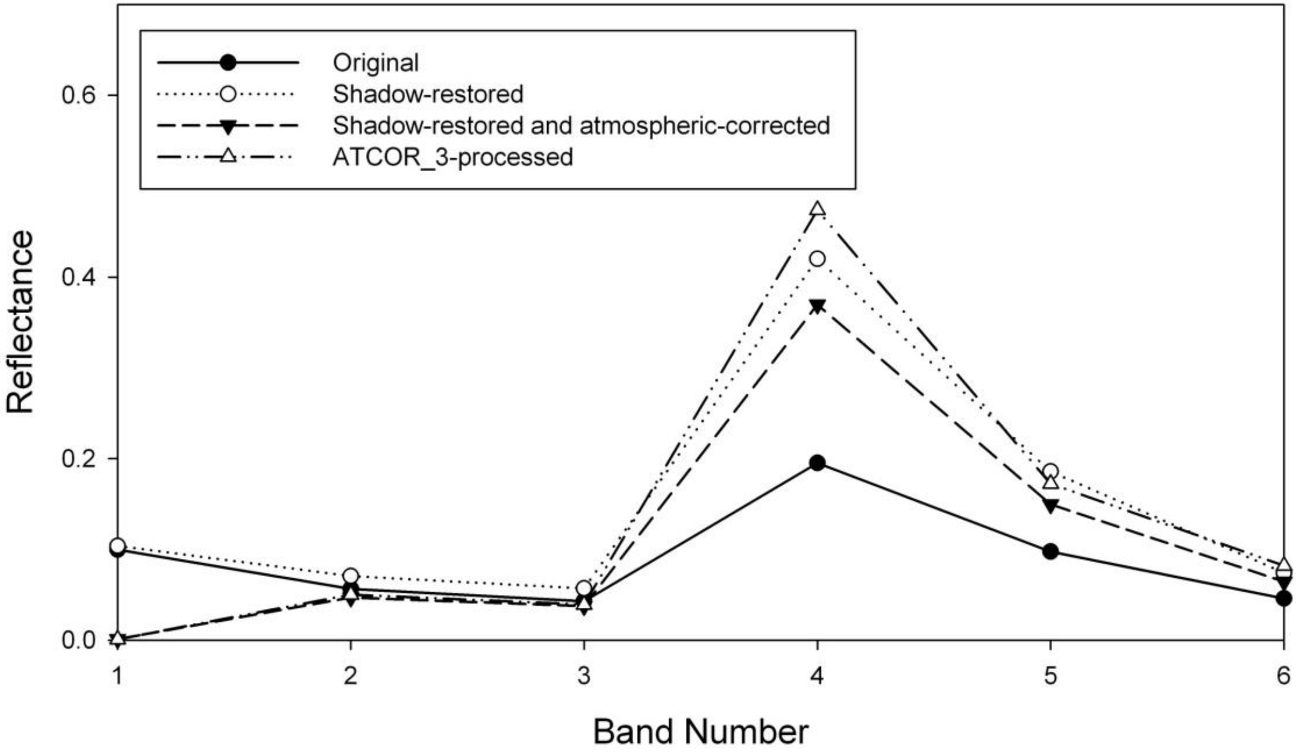

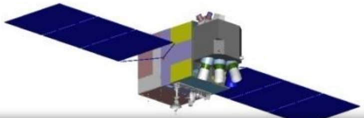

4

山体阴影信息恢复

Experiments on other areas

Origin

Topographic correction (DEM:30m)

CR method

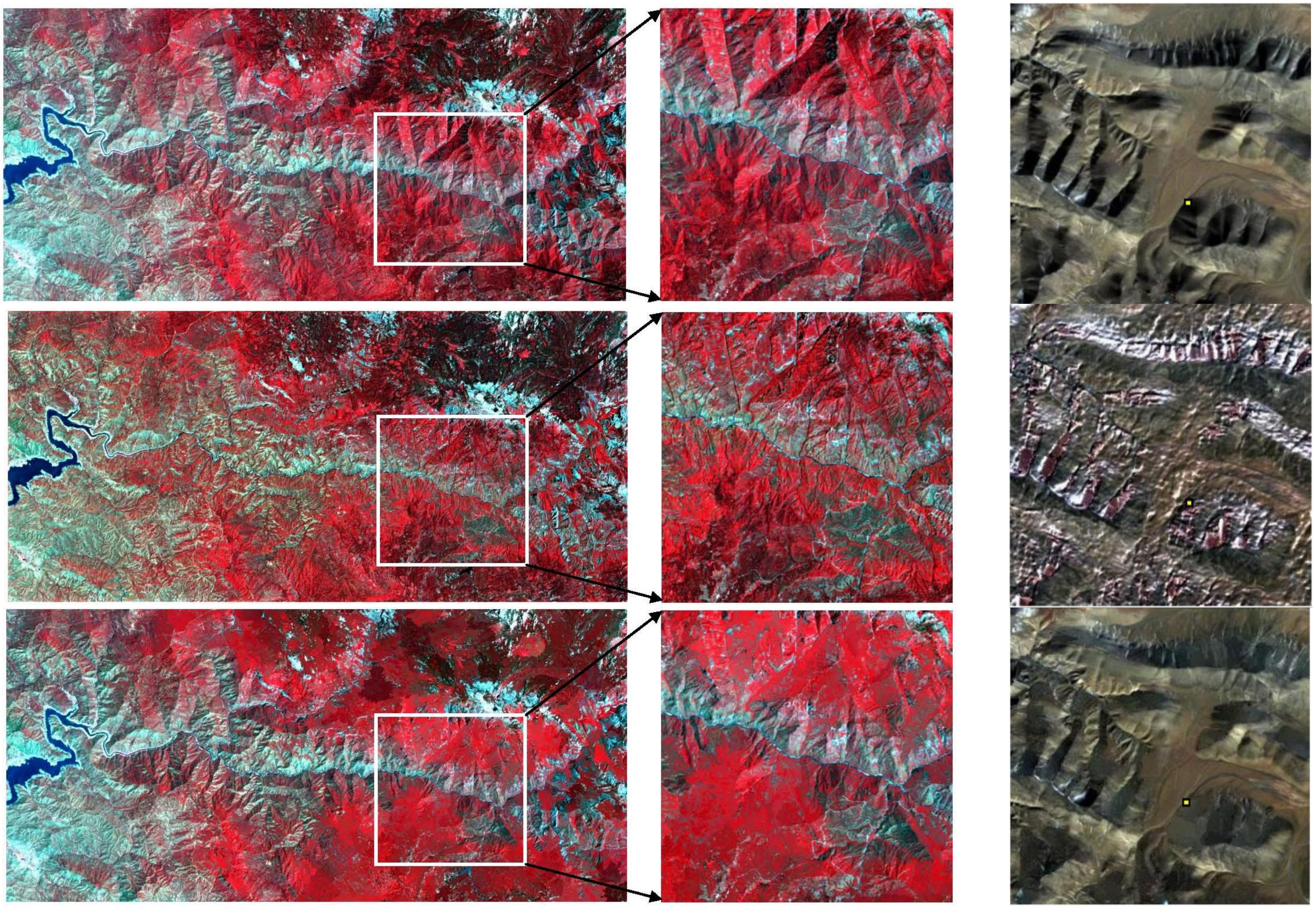

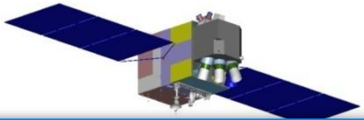

4 山体阴影信息恢复

Validation

Image	Class	Green	Red	NIR	SWIR
Atmospheric-corrected	Forest	2.9199	1.8996	5.2346	4.0026
	Barren land	3.5224	3.7294	3.6909	3.6512
ATCOR_3-processed	Forest	2.4297	1.2300	4.0510	3.0217
	Barren land	1.9278	2.9292	3.2567	2.6381
Shadow-restored & Atmospheric-corrected	Forest	1.7374	0.4061	2.9092	2.4359
	Barren land	1.9036	2.2798	0.9137	0.9177

4 山体阴影信息恢复

Land cover classification

Origin | Topographic correction | CR method

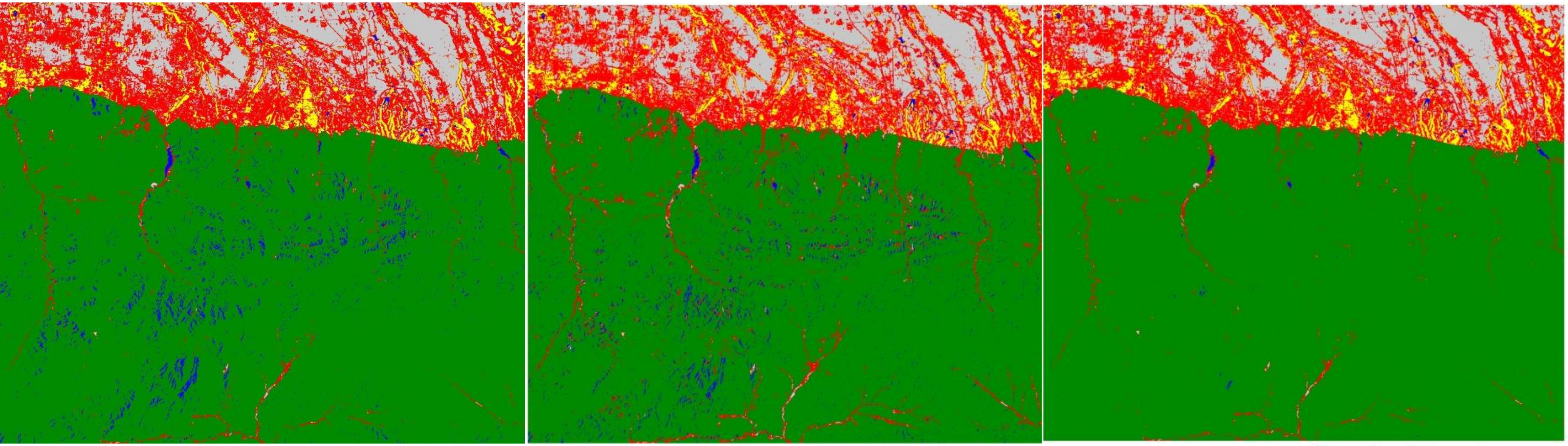

OA=75.97%
Kappa=0.6913

OA=77.85%
Kappa=0.7109

OA=86.93%
Kappa=0.8235

Forest
Crop land
Water
Urban land
Barren land

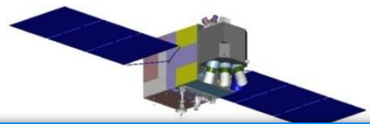

4 山体阴影信息恢复

- Texture analysis
  - Window size: 5×5
  - Indicator: Coefficient of Variance (CV)=standard deviation/mean

Image	Green	Red	NIR	SWIR
Atmospheric-corrected	0.0846	0.1334	0.0857	0.1543
ATCOR_3-processed	0.0786	0.1017	0.0762	0.1404
Shadow-restored & Atmospheric-corrected	0.0784	0.0946	0.0719	0.1230

  - CR method achieves the smallest CV, indicating the most homogeneous image. For mountainous areas dominated by homogeneous vegetation, the results clearly show the effect of CR and its advantage over topographic correction.

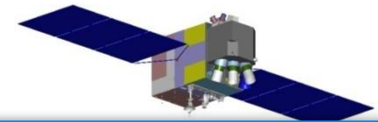

4 山体阴影信息恢复

This research proposes a new method to restore the radiometric information of shaded pixels of mountainous terrain in Landsat TM/ETM+ images without the aid of DEM data.

Through simulated spectral assessment and classification experiments on Landsat TM images, the proposed method was demonstrated to show improved spectral quality and classification accuracy compared to the original image and the topographically corrected one.

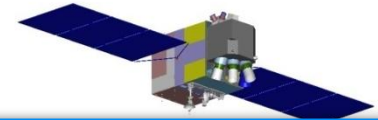

4 山体阴影信息恢复

CR method makes full use of the relationship between shaded pixels and their neighboring pixels with the similar spectral shape;

CR doesn't require DEM data, naturally avoiding the errors originating from this type of data, such as resampling and geometric registration;

Image segmentation: not only reduce the "salt and pepper" effect of shaded pixels, but also makes it possible to search for non-shaded similar pixels within the buffer area around each shaded object, speeding up the search process.

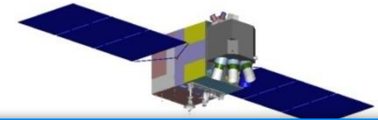

5 MODIS/Landsat数据融合

Temporal Continuous SR:

- Problem
  - The 16-day revisit cycle of Landsat has limited its use for studying global biophysical processes (16-day, 30m)
  - At the same time, MODIS scans whole Earth once or twice each day. However, the coarse resolution limit its ability in heterogeneous landscapes (daily, 250m & 500m)
- A Fusion Solution
  - To combine the spatial resolution of Landsat with the temporal frequency of coarse-resolution sensors, such as MODIS.

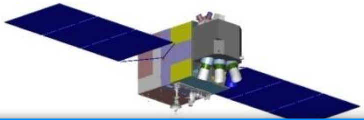

5 MODIS/Landsat数据融合

Spatial and Temporal Adaptive Reflectance Fusion Model:

- Objectives:
  - Fuse high-frequency temporal information from MODIS and high spatial resolution information from Landsat to produce “daily” Landsat-like surface reflectance

MODIS SR	1	2	3	4
Landsat SR	1			4

- Input:
  - MODIS and Landsat surface reflectance pair at tk
  - MODIS surface reflectance M(xi,yj,t0) at prediction date
- Predict:
  - Landsat surface reflectance L(xi,yj,t0) at prediction date

Gao, F., J. Masek, M. Schwaller and H. Forrest, On the Blending of the Landsat and MODIS Surface Reflectance: Predict Daily Landsat Surface Reflectance, IEEE Transactions on Geoscience and Remote Sensing, vol. 44, no. 8, pp. 2207-2218, 2006

5 MODIS/Landsat数据融合

Existing methods

- Traditional Image fusion methods (HIS, PCS) can **combine high-resolution panchromatic data with multispectral observations** acquired **simultaneously**;
- STARFM：Gao(2006) blended Landsat and MODIS data for predicting daily surface reflectance at Landsat spatial resolution，**failed in heterogeneous area**，cannot keep the spatial details.

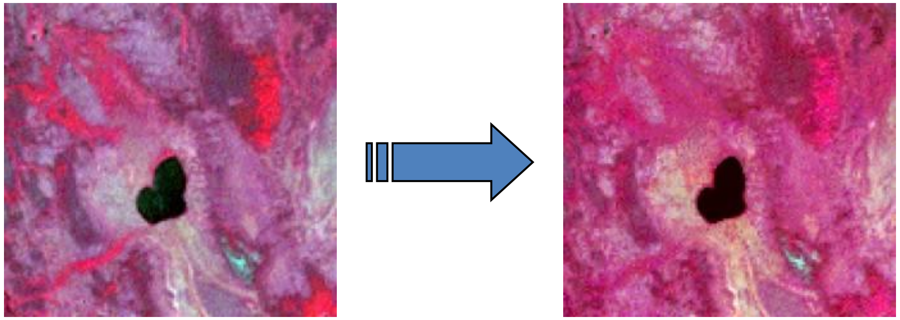

Ture image　　　Rebuilt by STARFM

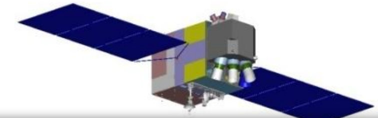

5 MODIS/Landsat数据融合

Theoretical basis

- **Pure coarse-resolution pixel** ：the difference between the MODIS and Landsat is only caused by the systematic biases

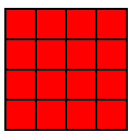

$$F(x,y,t_0,B) = a \times C(x,y,t_0,B) + b$$

$$F(x,y,t_p,B) = a \times C(x,y,t_p,B) + b.$$

$$F(x,y,t_p,B) = F(x,y,t_0,B) + a \times (C(x,y,t_p,B) - C(x,y,t_0,B)).$$

- **Mixed coarse-resolution pixel**: based on spectral linear mixing model and the assumption the reflectance change is stable for every land cover type during a short period

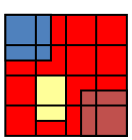

$$C_m = \sum_{i=1}^{M} f_i\left(\frac{1}{a}F_{im} - \frac{b}{a}\right) + \varepsilon$$

$$C_n = \sum_{i=1}^{M} f_i\left(\frac{1}{a}F_{in} - \frac{b}{a}\right) + \varepsilon$$

$$F_{in} = h_i \times \Delta t + F_{im}$$

$$\rightarrow \quad \frac{F_{kn} - F_{km}}{C_n - C_m} = \frac{h_k}{\sum_{i=1}^{M} \frac{f_i h_i}{a}} = v_k.$$

$$\downarrow$$

$$F(x,y,t_p,B) = F(x,y,t_0,B) + v(x,y) \times (C(x,y,t_p,B) - C(x,y,t_0,B)).$$

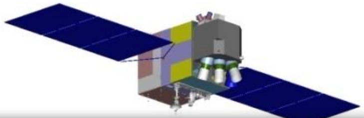

5 MODIS/Landsat数据融合

Theoretical basis

- Considering the spatial consistency of reflectance change, A **moving window** method is thus used to take full advantage of the information from neighbor pixels, especially the information from pure pixels

$$F(x_{w/2}, y_{w/2}, t_p, B) = F(x_{w/2}, y_{w/2}, t_0, B) + \sum_{i=1}^{N} W_i \times V_i \times (C(x_i, y_i, t_p, B) - C(x_i, y_i, t_0, B))$$

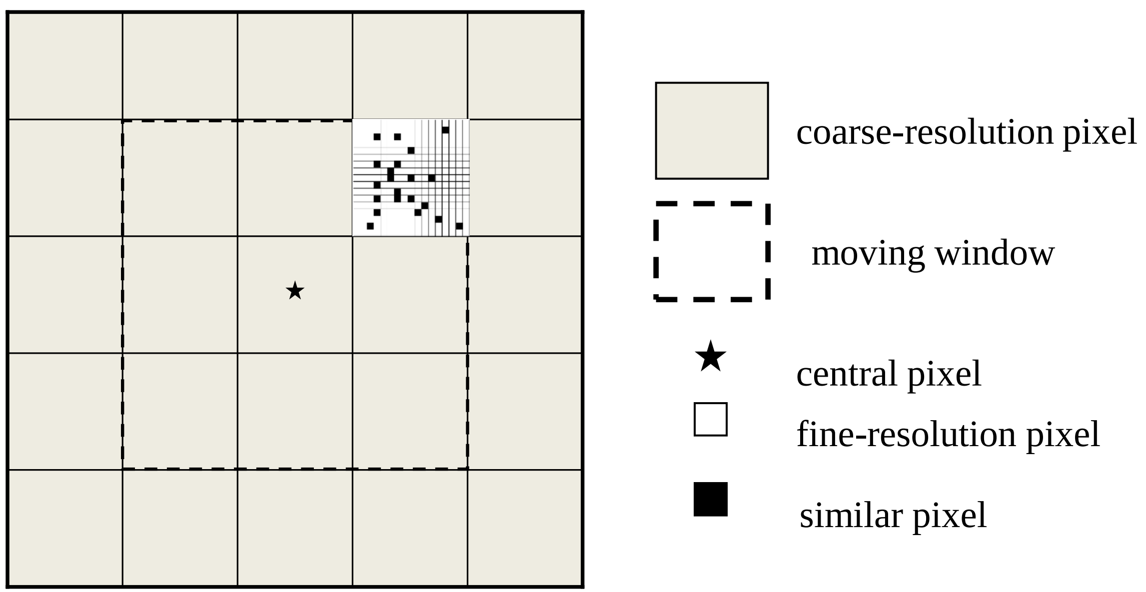

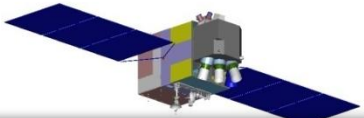

5 MODIS/Landsat数据融合

- Process of implementation
  - Flowchart

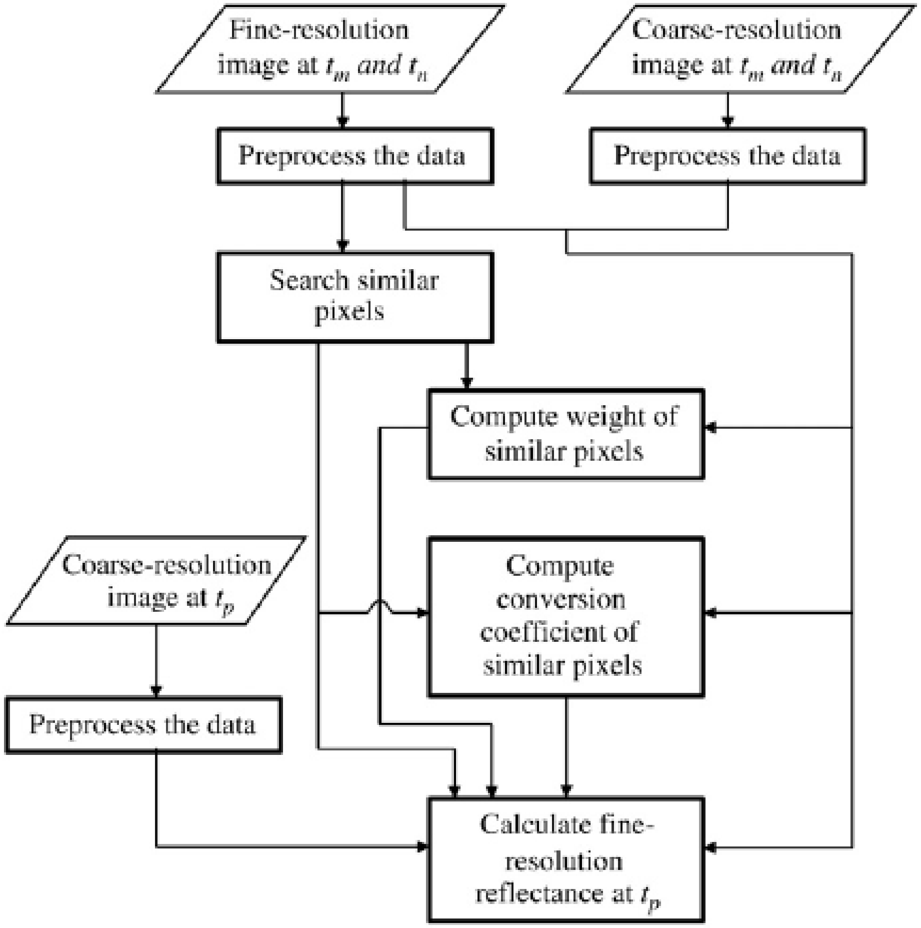

Fig. 1. The flowchart of the ESTARFM algorithm.

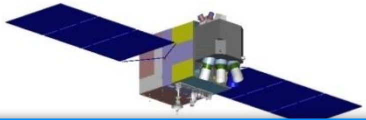

5 MODIS/Landsat数据融合

Step 1 Step 2 Step 3 Step 4

Selection of similar neighbor pixels

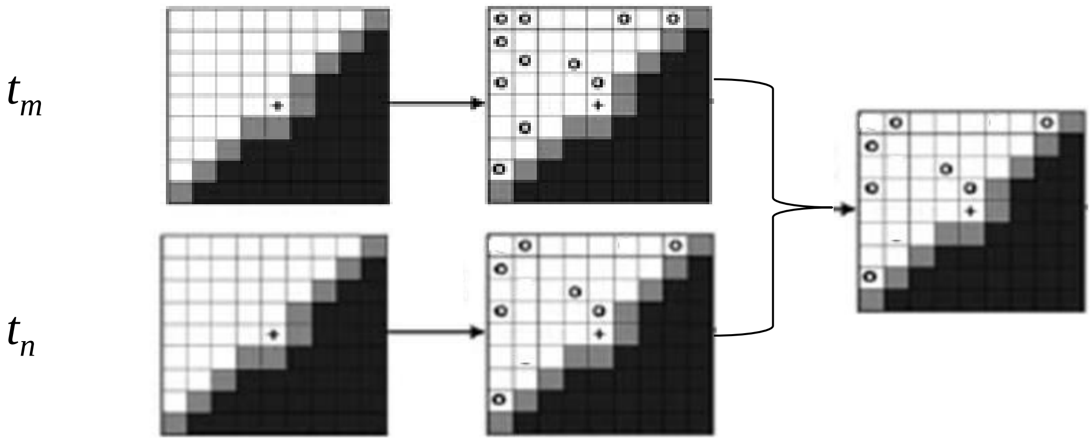

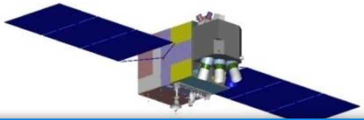

5 MODIS/Landsat数据融合

Step 1 | Step 2 | Step 3 | Step 4

Calculation of weight for similar pixels, consider spectral similarity and spatial distance

$$R_i = \frac{E[(\mathbf{F}_i - E(\mathbf{F}_i))(\mathbf{C}_i - E(\mathbf{C}_i))]}{\sqrt{D(\mathbf{F}_i)} \cdot \sqrt{D(\mathbf{C}_i)}} \quad d_i = 1 + \sqrt{(x_{w/2} - x_i)^2 + (y_{w/2} - y_i)^2} / (w/2)$$

$$\mathbf{F}_i = \{F(x_i, y_i, t_m, B_1), \ldots, F(x_i, y_i, t_m, B_n), F(x_i, y_i, t_n, B_1), \cdots, F(x_i, y_i, t_n, B_n)\}$$

$$\mathbf{C}_i = \{C(x_i, y_i, t_m, B_1), \cdots, C(x_i, y_i, t_m, B_n), C(x_i, y_i, t_n, B_1), \cdots, C(x_i, y_i, t_n, B_n)\}$$

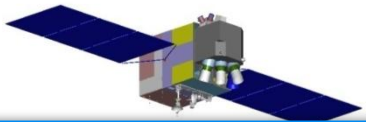

5 MODIS/Landsat数据融合

Step 1 | Step 2 | **Step 3** | Step 4

Calculation of conversion coefficient ： apply linear regression model

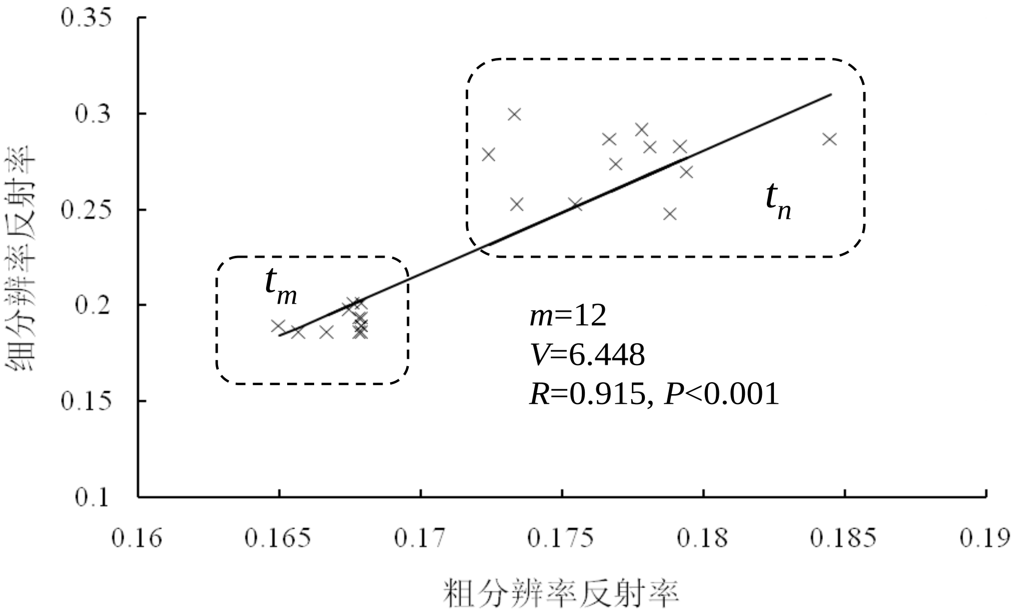

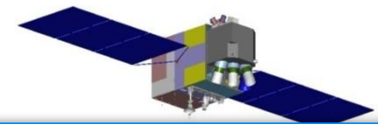

5

MODIS/Landsat数据融合

Step 1 Step 2 Step 3 **Step 4**

Calculation of reflectance of the central pixel

$$T_k = \frac{1/\left|\sum_{j=1}^{w}\sum_{l=1}^{w} C(x_j, y_l, t_k, B) - \sum_{i=1}^{w}\sum_{l=1}^{w} C(x_j, y_l, t_p, B)\right|}{\sum_{k=m,n}\left(1/\left|\sum_{j=1}^{w}\sum_{l=1}^{w} C(x_j, y_l, t_k, B) - \sum_{i=1}^{w}\sum_{l=1}^{w} C(x_j, y_l, t_p, B)\right|\right.}, (k = m, n)$$

$$F(x_{w/2}, y_{w/2}, t_p, B) = T_m \times F_m(x_{w/2}, y_{w/2}, t_p, B) + T_n \times F_n(x_{w/2}, y_{w/2}, t_p, B)$$

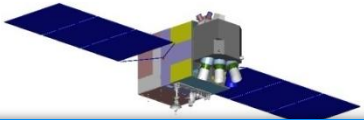

5 MODIS/Landsat数据融合

Tests with simulated data (Small)

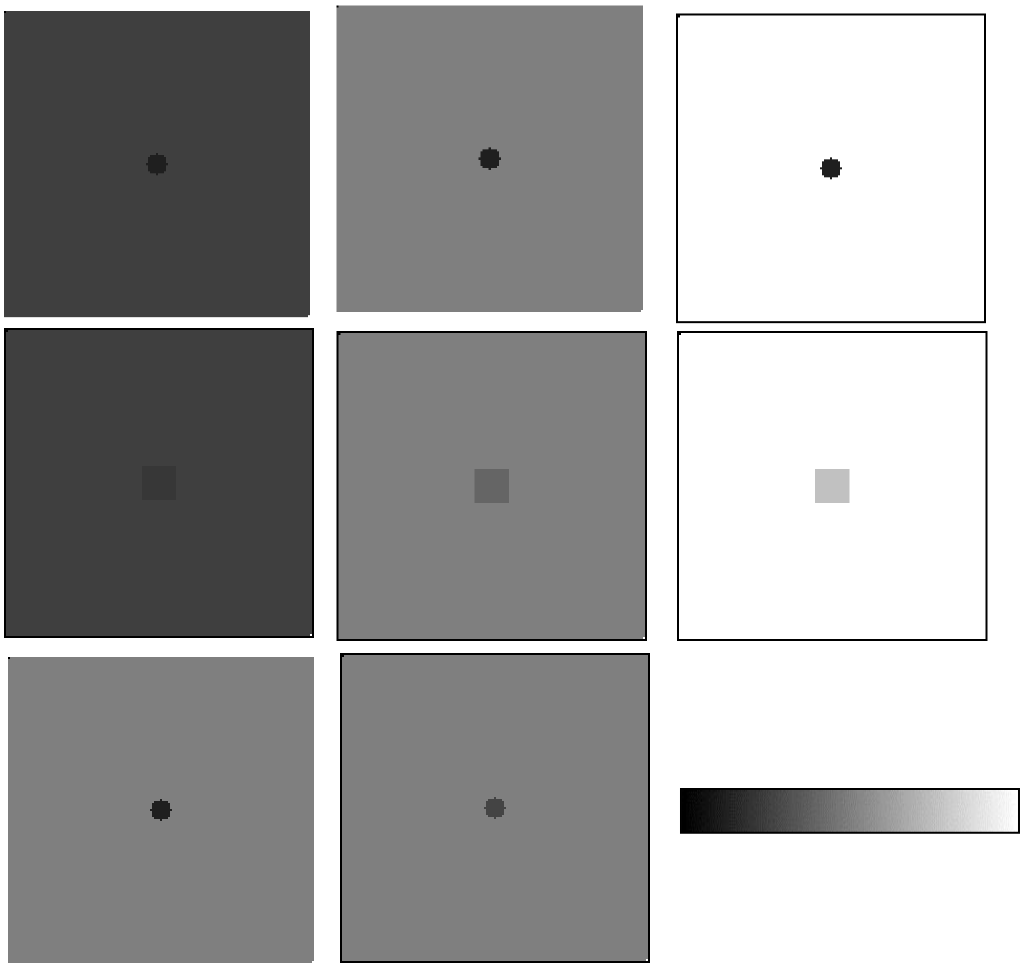

TM

MODIS

ESTARFM STARFM

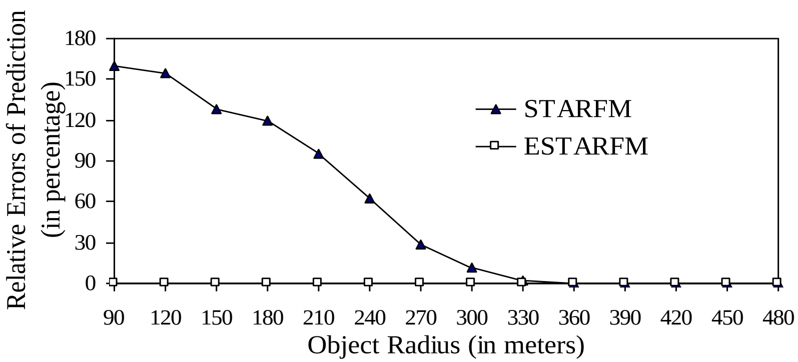

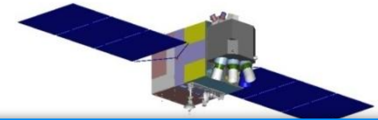

5 MODIS/Landsat数据融合

Tests with simulated data (Linear)

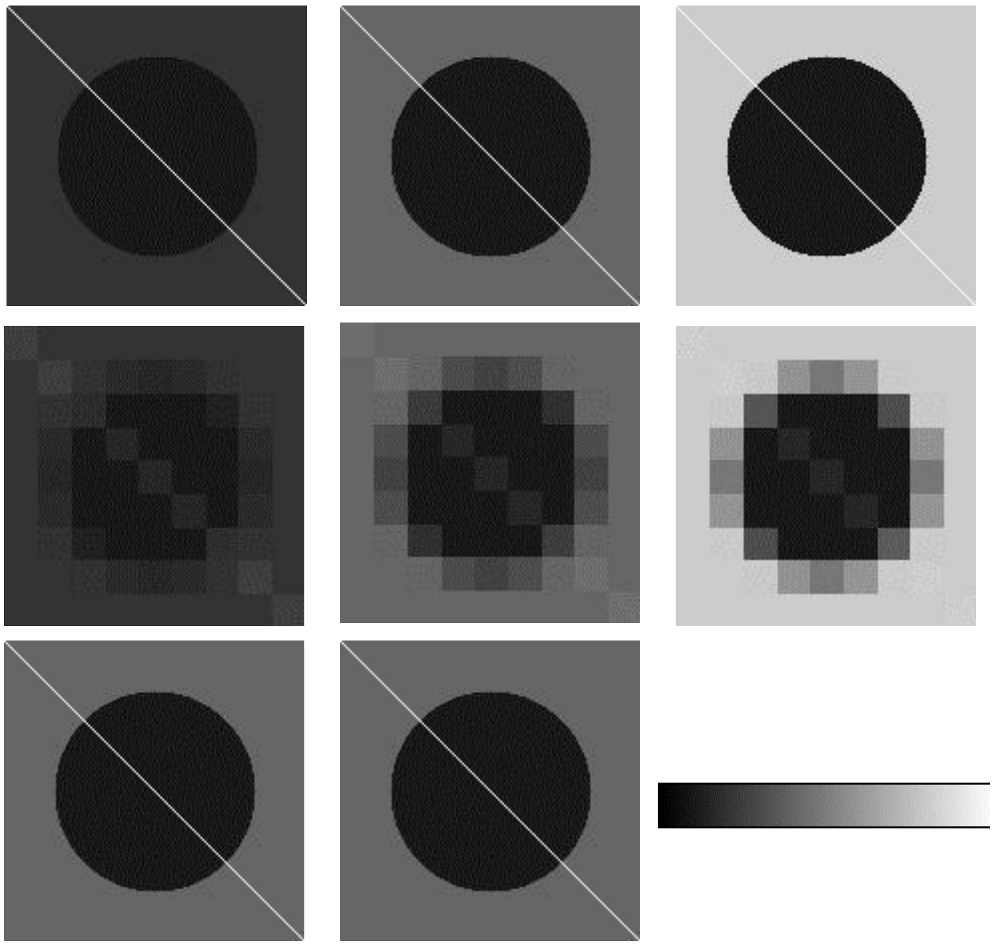

TM

MODIS

ESTARFM STARFM

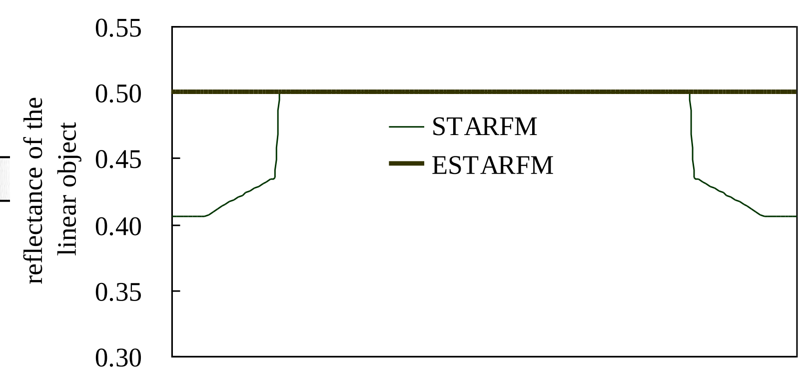

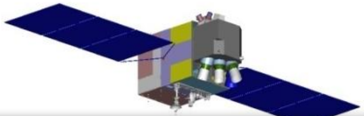

5 MODIS/Landsat数据融合

Tests with satellite data (Seasonal Changes over Forest)

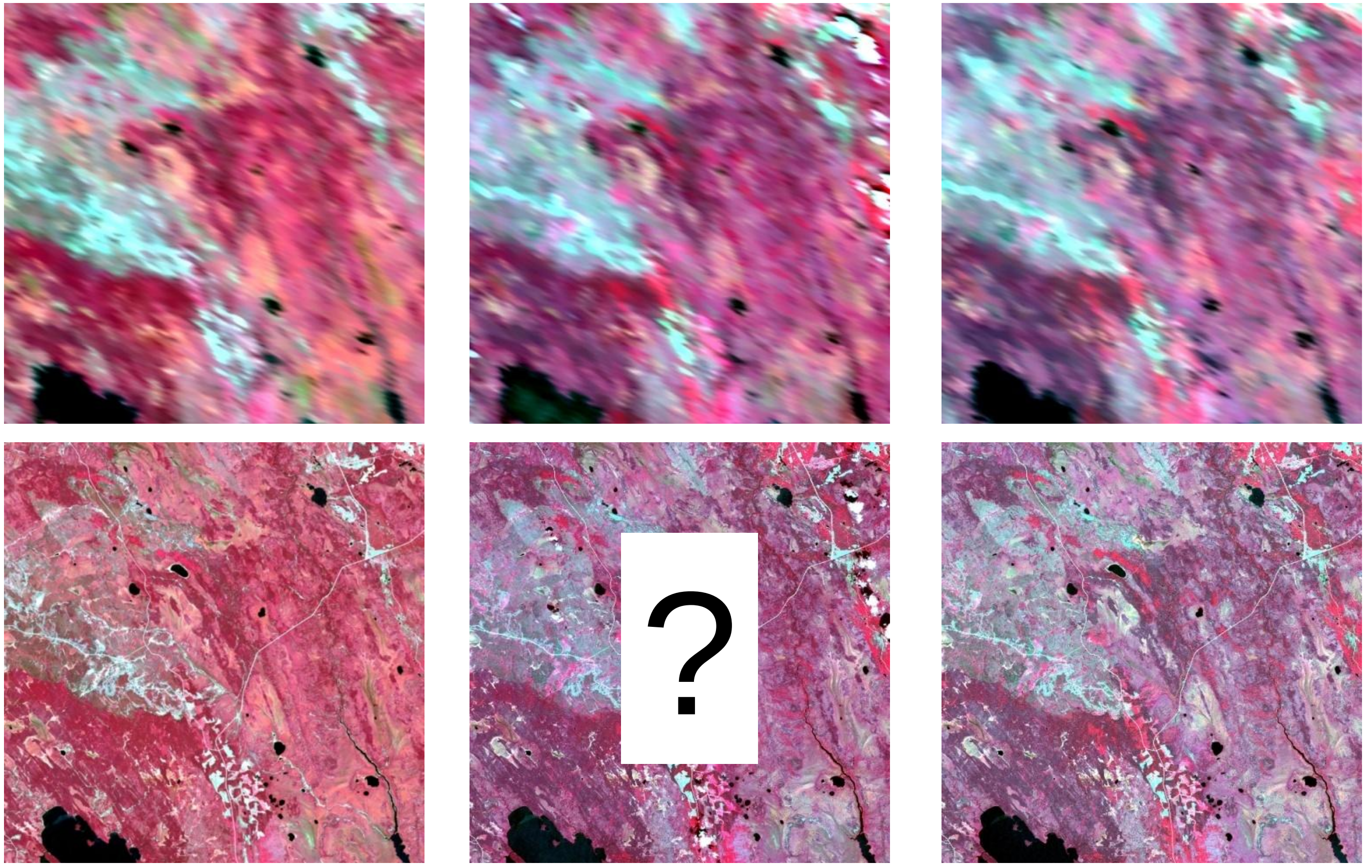

5/24/01 7/11/01 8/12/01

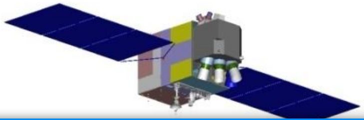

5 MODIS/Landsat数据融合

Tests with satellite data (Seasonal Changes over Forest)

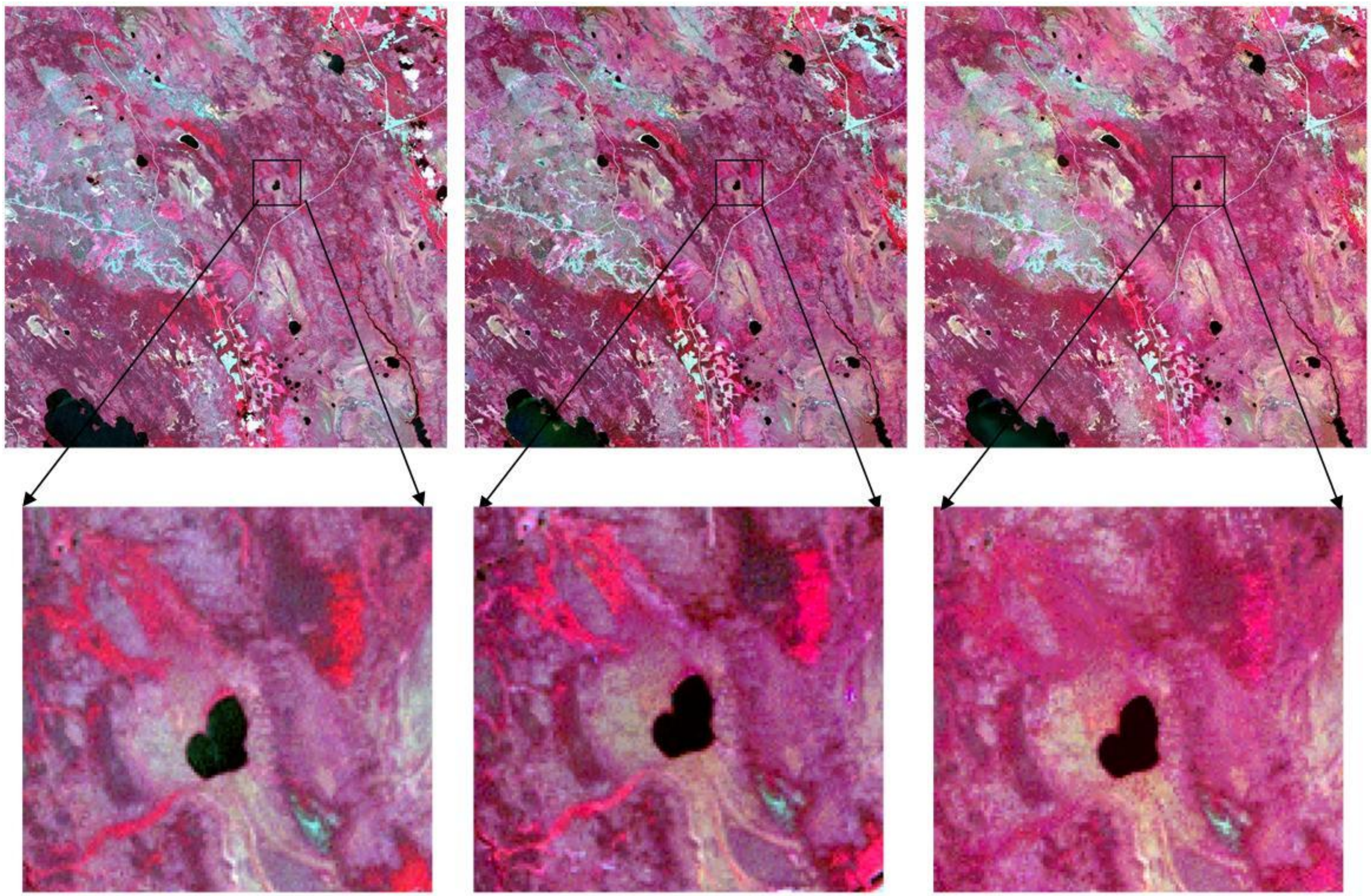

(a)True image (b) ESTARFM (c) STARFM

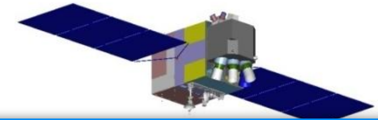

5 MODIS/Landsat数据融合

Tests with satellite data (Seasonal Changes over Forest)

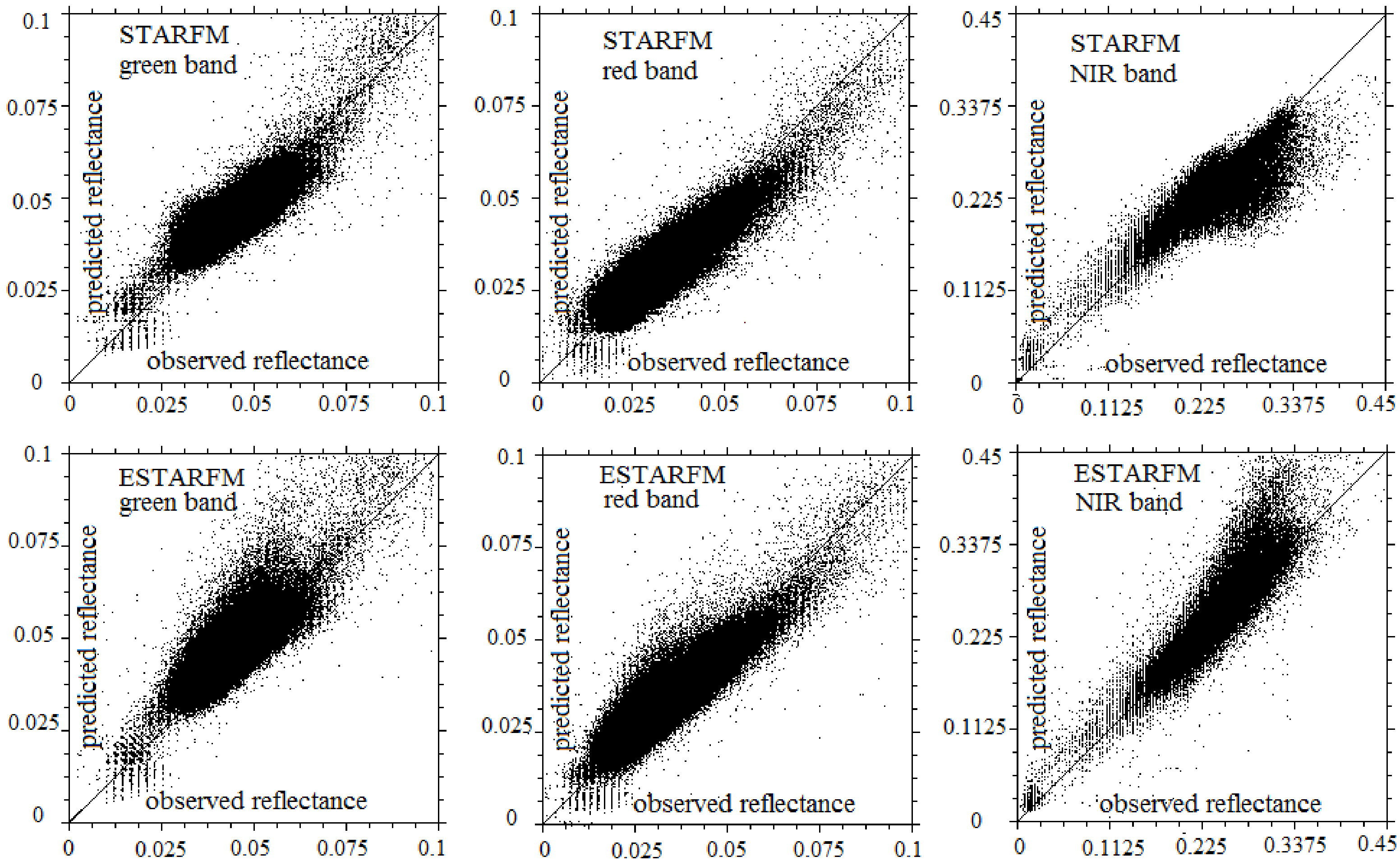

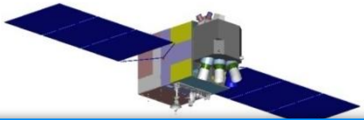

5 MODIS/Landsat数据融合

Tests with satellite data (Seasonal Changes over Forest)

ETM+	Average Absolute Difference (AAD)				Average Difference (AD)			
Band	5/24/01	8/12/01	Prediction		5/24/01	8/12/01	Prediction	
			STARFM	ESTARFM			STARFM	ESTARFM
green	0.0043	0.0071	0.0035	0.0035	-0.0014	0.0070	-0.0002	-0.0009
red	0.0114	0.0058	0.0044	0.0032	-0.0111	0.0053	0.0012	0.0002
NIR	0.0443	0.0155	0.0129	0.0106	0.0441	0.0140	-0.0030	-0.0041

ESTARFM is more accurate.

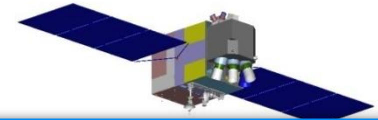

5 MODIS/Landsat数据融合

Tests with satellite data (Complex Mixture Region)

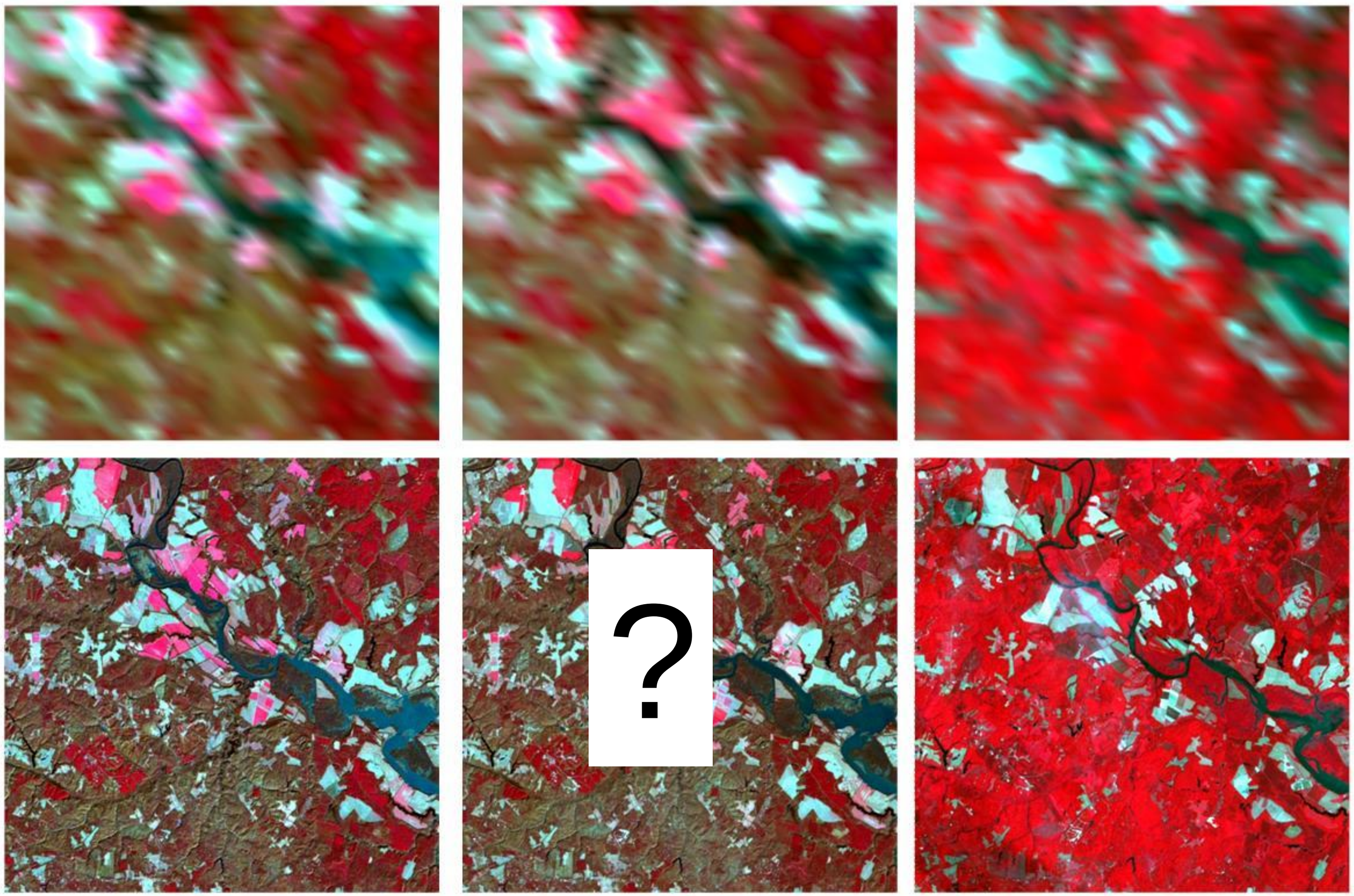

1/25/02 2/26/02 5/17/02

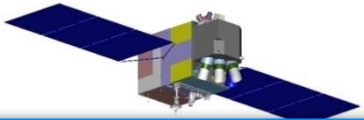

5 MODIS/Landsat数据融合

Tests with satellite data (Seasonal Changes over Forest)

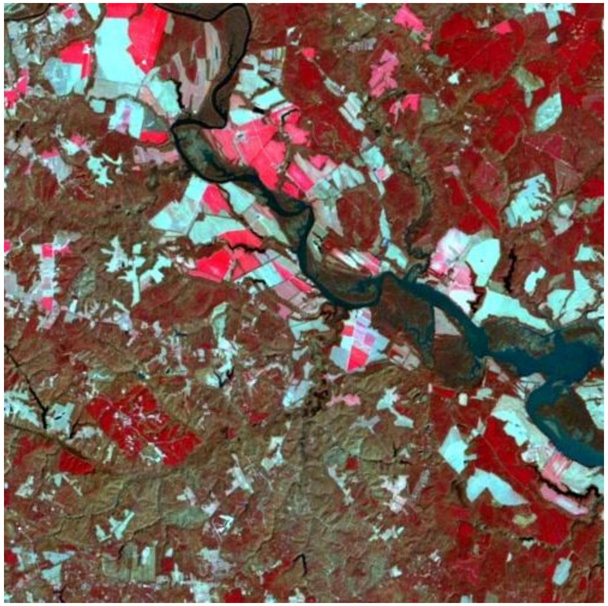

(a) True image

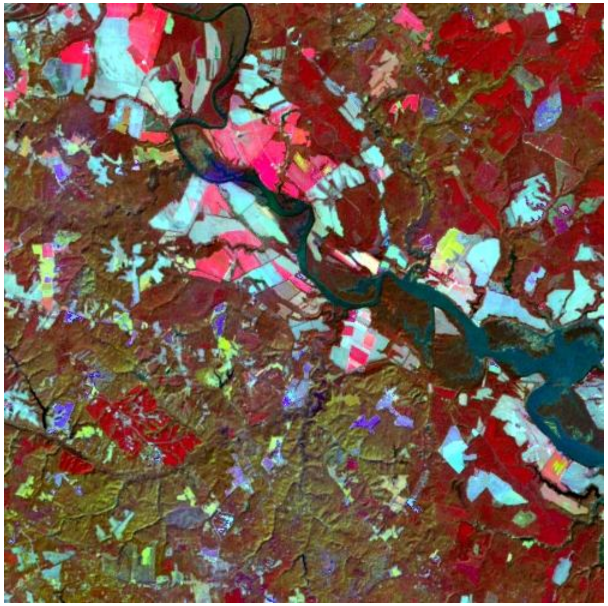

(b) ESTARFM

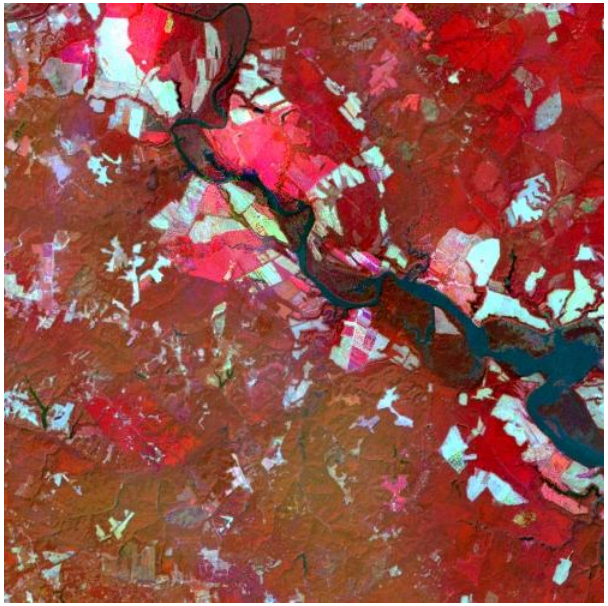

(c) STARFM

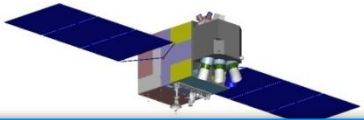

5 MODIS/Landsat数据融合

Tests with satellite data (Seasonal Changes over Forest)

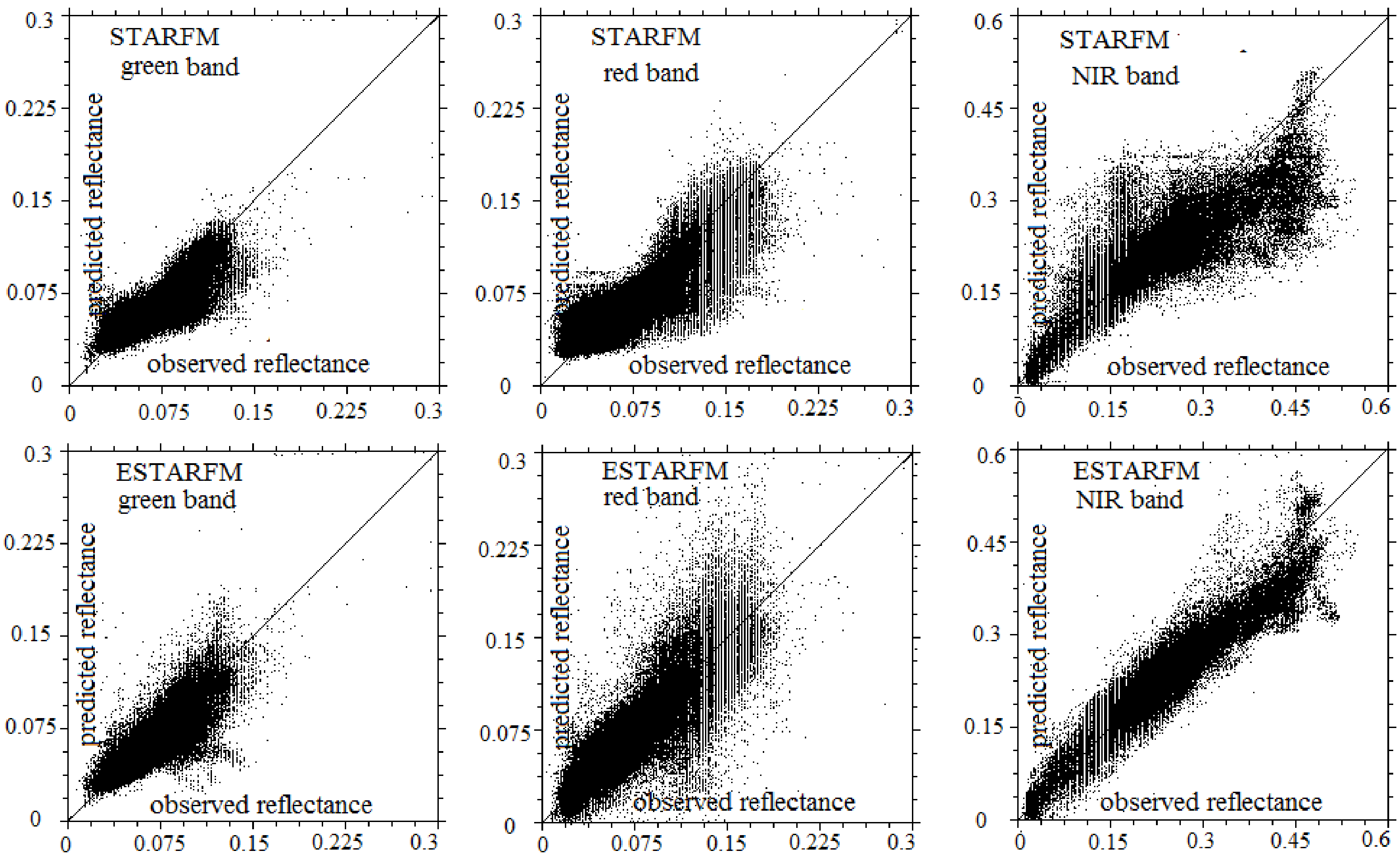

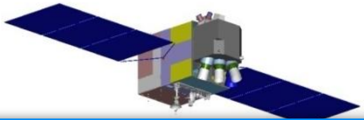

5 MODIS/Landsat数据融合

Tests with satellite data (Seasonal Changes over Forest)

ETM+	Average Absolute Difference (AAD)				Average Difference (AD)			
			Prediction				Prediction	
Band	1/25/02	5/17/02	STARFM	ESTARFM	1/25/02	5/17/02	STARFM	ESTARFM
green	0.0119	0.0107	0.0075	0.0068	0.0113	-0.0031	0.0026	0.0028
red	0.0150	0.0283	0.0111	0.0095	0.0143	0.0218	0.0040	0.0021
NIR	0.0279	0.1774	0.0196	0.0135	0.0269	-0.1722	0.0060	0.0022

ESTARFM improved the accuracy more in heterogeneous area.

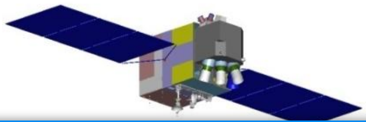

5 MODIS/Landsat数据融合

Comparing with the original STARFM algorithm, it can produce the synthetic fine-resolution reflectance product more accurately, especially for heterogeneous landscapes.

The improvements includes using a conversion coefficient, intersection of similar pixels selection, using spectral similarity, weighting the change rather than final prediction of each similar pixel.

Limitations : cannot accurately predict the shapes changes; Sensors with different band passes may lead to nonlinear relationship; the assumption that reflectance linear change is constant might be not available during a long period; more computational cost than STARFM.

The end

Thanks for your attention!